

Spatiotemporal analysis of different vegetation indices and relation to meteorological parameters over a tropical urban location and its surroundings

Arijit DE^{1*}, Nemai SAHANI², Abhirup DATTA³ and Animesh MAITRA⁴

¹*Department of Electromagnetic and Radar, ONERA, The French Aerospace Lab, 91120 Palaiseau, France.*

²*Independent Researcher, West Bengal, India.*

³*DAASE, Indian Institute of Technology Indore, 453552, Madhya Pradesh, India.*

⁴*Institute of Radio Physics and Electronics, University of Calcutta, 700009, West Bengal, India.*

*Corresponding author; email: arijide0303@gmail.com

Received: May 27, 2023; Accepted: April 2, 2024

RESUMEN

Este artículo investiga las características espaciotemporales a largo plazo de varios índices de vegetación (VI, por su sigla en inglés) derivados de satélites, como el índice normalizado de vegetación diferenciada (NDVI) y el índice de vegetación mejorado (EVI), así como la productividad primaria bruta (GPP) y la fluorescencia de clorofila inducida por el sol (SIF) en la conurbación de Calcuta y sus áreas circundantes de 2003 a 2016. Además, analiza la correlación entre estos índices de vegetación y parámetros atmosféricos como la lluvia, la humedad del suelo (SM), la evapotranspiración (ET) y la temperatura de la superficie terrestre (LST). Se observan las variaciones mensuales de estos parámetros y se examina la variabilidad interanual mediante técnicas de regresión lineal. El estudio también observa la correlación espacial promedio temporal entre los VI y los parámetros climáticos. Además, investiga el efecto del desfase temporal utilizando el análisis del coeficiente de correlación de Pearson entre el VI y otros parámetros meteorológicos (0, 1, 2 y 3 meses). El NDVI y el EVI exhiben una correlación máxima con la lluvia, SM, ET y LST dentro de períodos de retraso específicos; asimismo, muestran una lenta tasa de respuesta a la lluvia y su sensibilidad depende de la SM y la ET. Se observa una correlación positiva entre el NDVI y la ET, lo que indica que el primero aumenta con el agua vaporizada en la atmósfera. Se observa una correlación negativa entre NDVI y LST en la región estudiada. Los conocimientos del estudio son valiosos para predecir las características futuras del VI con base en parámetros meteorológicos en áreas urbanas tropicales como Calcuta y sus alrededores. Esta capacidad predictiva puede ayudar a mitigar los efectos climáticos adversos sobre la vegetación.

ABSTRACT

The paper investigates the long-term spatiotemporal characteristics of various satellite-derived vegetation indices (VI), such as the Normalized Difference Vegetation Index (NDVI) and Enhanced Vegetation Index (EVI), as well as Gross Primary Productivity (GPP) and Sun-induced Chlorophyll Fluorescence (SIF) over the Kolkata conurbation and its surrounding areas from 2003 to 2016. Additionally, it analyzes the correlation between these vegetation indices and atmospheric parameters like rainfall, soil moisture (SM), evapotranspiration (ET), and land surface temperature (LST). Monthly variations of these parameters are observed, and inter-annual variability is examined using linear regression techniques. The study also observes the time average spatial correlation between vegetation indices and weather parameters. Moreover, it investigates the time-lag effect (0, 1, 2, and 3 months) using Pearson correlation coefficient analysis between VI and other meteorological parameters. NDVI and EVI exhibit maximum correlation with rainfall, SM, ET, and LST within specific lag periods. NDVI and EVI show a slow response rate to rainfall, and their sensitivity depends on SM and ET. A positive correlation is observed between NDVI and ET, indicating that NDVI increases with vaporized water in the atmosphere. A negative correlation is noted between NDVI and LST

in the region studied. The study's insights are valuable for predicting future vegetation index characteristics based on meteorological parameters in tropical urban areas like Kolkata and its surroundings. This predictive capability can aid in mitigating adverse weather effects on vegetation.

Keywords: satellite data, spatiotemporal analysis, vegetation index, meteorological parameters, urban location, linear regression, correlation.

1. Introduction

Vegetation indices (VI) are the foremost important metrics to watch ecosystem and land surface processes (Nicholson et al., 1990; Ichii et al., 2002; Wang et al., 2003; Gu et al., 2008). Vegetation changes play an essential role in the environmental process. They are a decent indicator of climate, hydrology, energy balance, and hydrological cycles (Nicholson et al., 1990; Farrar et al., 1994). Recent research suggests that environmental changes, particularly climate change, have led to decreased food security and vegetation cover alterations (Akram et al., 2018; Ali et al., 2019; Din et al., 2022). The ecosystem and vegetation are changing due to climate change (Fahad et al., 2017; Hateffard et al., 2021). The knowledge regarding the long-term variation of VI plays a vital role in determining the climate change pattern and monsoon variability (Amin et al., 2017; Baqa et al., 2022). The interconnectedness of vegetation cover with various ecological processes such as the energy cycle, hydrology, and climate has also been discussed in several studies (Hussain et al., 2020a; Masood et al., 2022; Chandra et al., 2023, De et al., 2023). The role of vegetation in mitigating climate change effects and its importance in studying plant phenology and biomass are also emphasized in literature (Feizizadeh et al., 2013; Sabr et al., 2016; Hassan et al., 2021; Karuppasamy et al., 2022; Naz et al., 2022; Hussain et al., 2023a; Yang et al., 2023a, b). These findings underscore the importance of understanding and monitoring vegetation dynamics in the context of climate change and food security.

The Normalized Difference Vegetation Index (NDVI) is one of the most recognized and commonly used parameters to review vegetation cover and crop health (Sellers et al., 1986; Piao et al., 2003). It indicates the greenness of the land surface and, therefore, vegetation density (Choubin et al., 2017; Sajedi-Hosseini et al., 2018). The Enhanced Vegetation Index (EVI) is another parameter that minimizes canopy-soil variations and improves

sensitivity over dense vegetation conditions. The NDVI serves as a valuable tool in monitoring vegetation health and dynamics due to its correlation with chlorophyll content and leaf area index and has wide application in assessing land use/land cover changes (LULC), detecting crop types, estimating crop yield and production, among others (Sultana et al., 2014; Rani et al., 2018, Tariq et al., 2020). NDVI values are indicative of the biological activities of plants and can effectively characterize changes in active surface temperature, providing insights into vegetative cover conditions (Zahoor et al., 2019; Aslam et al., 2021). While the NDVI is particularly sensitive to chlorophyll activity, EVI complements it by capturing structural differences in plants, making it especially useful for delineating tropical forests. Together, NDVI and EVI contribute significantly to our understanding of vegetation dynamics and ecosystem health (Matsushita et al., 2007; Waleed et al., 2022; Vélez et al., 2023).

The variation of different vegetation indices and their relationship with various climatic parameters is vital to understanding the effect of climate change on vegetation expansion. It has been evident that both NDVI (Rouse, 1974) and EVI have a reference to rainfall (Liu and Huete, 1995; Potter and Brooks, 1998; Richard and Poccard, 1998; Wu et al., 2016). The satellite-derived vegetation index is a well-accepted and primarily used method to explore the response of vegetation over a location (Tucker, 1979; Piao et al., 2011; Zhang et al., 2013).

In recent years, satellite-derived vegetation index has been a crucial tool to assess vegetation dynamics at regional to global scales (Myndeni et al., 1997; Zhao et al., 2012; Cleland et al., 2006; Schwartz et al., 2006; Ssemmanda et al., 2014; Cao et al., 2018). Satellite-derived NDVI data is a crucial indicator for analyzing the growth of green vegetation and the effect of climate change on vegetation dynamics (Walther et al., 2002; Zhang et al., 2002; Yu et al., 2003; Piao et al., 2006; Philippon et al., 2007;

Zhao et al., 2015). It has been seen that the spatial patterns of annually integrated NDVI closely reflect the mean annual rainfall over East Africa and the Sahel (Nicholson et al., 1990). An increase in NDVI was evident in Tanzania from 1982 to 1994, as seen in NDVI imagery (Pelkey et al., 2000).

The intricate relationship between global warming, vegetation cover, and various environmental processes has been discussed by many authors. Global warming, attributed largely to human activities since the Industrial Revolution, has increased land surface temperature (LST). This temperature rise has significant implications for vegetation cover, as outlined by various studies (Nasim et al., 2018; Hussain et al., 2020a, b; Mubeen et al., 2021; Akram et al., 2022). The rise in temperature and decreased precipitation results in more drought conditions and reduced vegetation in Kenya (Ogutu et al., 2008). It has been observed that various weather parameters like precipitation, land surface temperature (LST), soil moisture (SM), and solar radiation significantly impact vegetation growth (Lakshmi and Barbosa, 2012). The regression analysis findings over the Sahiwal region, Pakistan, indicate a significant relationship between LST values and both the Normalized Difference Vegetation Index (NDVI) and Enhanced Vegetation Index (EVI). Specifically, where LST values are lower, NDVI and EVI values tend to be higher and more significant. Conversely, in areas with higher LST values, NDVI and EVI values are lower (Hussain, et al., 2023b). A negative correlation between the NDVI and temperature has been observed in north China (Yang et al., 2023b). The yearly and seasonal variation of NDVI and its relation to precipitation were observed over the Gojob River catchment from 1982 to 2015 (Dagnachew et al., 2020).

Together with human activities, environmental changes have a significant impact on vegetation (Sha et al., 2020). Long-term variation of vegetation dynamics has been discussed with the help of Advanced Very High Resolution Radiometer (AVHRR) sensors (Eastman et al., 2013). NDVI shows an upward trend with temperature and precipitation before the 1990s, whereas a downward trend in the NDVI has been observed since the mid or late 1990s. Landsat-7 ETM data has been used to find the relationship between NDVI and LST (Mallick et al., 2012; Senanayake et

al., 2013). The correlation values between NDVI and TST, SM, and precipitation are -0.45, 0.43, and 0.34, respectively, over Gautam Budha Nagar, India (Sharma et al., 2022). The long-term variation of precipitation and temperature and its effect on the annual crop production has been observed using Landsat data over India (Basistha et al., 2009; Kundu and Dutta 2011; Duhan and Pandey, 2013; Gautam et al., 2020; Dutta et al., 2015; Sahoo et al., 2015; Kundu et al., 2017). The precipitation value at each station has been interpolated using ArcGIS 9.3 to find the spatial variation of rainfall. Duhan et al. (2013) showed that mean annual precipitation has varied from 694 mm (at Westnimar) to 1416 mm (at Mandla). Kundu and Dutta (2011) demonstrated a varying pattern of vegetation dynamics in response to rainfall over the Bundelkhand area. Sahoo et al. (2015) found a good agreement between satellite-derived and meteorological drought indices. The effect of SM on vegetation growth has also been studied by Gao et al. (2014), who used a wireless sensor network to collect soil moisture data.

The significantly increasing trend in vegetation sensitivity to SM in many semi-arid and arid regions across the globe indicates a growing vulnerability of vegetation to changes in SM levels. This trend suggests that vegetation in these regions is becoming more responsive to variations in SM availability, which can have profound implications for ecosystem health, biodiversity, and the livelihoods of communities dependent on these ecosystems (Li et al., 2022). The observed strong positive correlation between SM and vegetation indices with an eight-week lag time over the USA corn belt suggests that changes in SM levels influence vegetation dynamics with a certain time delay (Adegoke and Andrew, 2002). Various techniques, such as discrete wavelet transform, artificial neural network, and feature extraction have been used to estimate the dynamical characteristics of NDVI (Demirel et al., 2010; Yamaguchi et al., 2010; Bhandaria et al., 2012). There are a few studies on the relation between EVI and weather parameters. It has been observed that EVI is the most effective vegetation index compared to in situ data over Asia during the monsoon season (Motohka et al., 2009). It has been observed that EVI can be a better index than NDVI for vegetation monitoring across various ecosystems, as it is insensitive to background

reflectance and a better predictor of gross primary productivity (GPP; Rocha and Shaver, 2009). A good correlation between EVI and rainfall and temperature has been observed, with time lag effect, in Zacatecas, Mexico (Olmos-Trujillo et al., 2020). The Moderate Resolution Imaging Spectrometer (MODIS) satellite-derived EVI has been used to estimate ET, which correlates well with the actual data. The polar-orbiting MODIS sensor aboard the Terra and Aqua platforms is well accepted for environmental monitoring of the vegetation indices (Huete et al., 2002). MODIS-derived VIs present improved estimations of spatial, spectral, and radiometric representations of surface vegetation conditions (Tucker et al., 2005; Lu et al., 2015).

This comprehensive study aims to understand the dynamics of VIs and their relationship with various weather parameters in Kolkata, India, and its surrounding region. The study offers valuable insights into the complex interactions between vegetation dynamics and environmental factors in the study region. Vegetation cover plays a crucial role in various aspects of the Earth's systems and processes, like hydrology and regional and global climate change, variations in the terrestrial ecosystem, soil ecosystems, and others. Overall, vegetation cover is a cornerstone of Earth's ecosystems, influencing human societies, biodiversity, ecosystem functions, and climate processes. Protecting and sustainably managing the vegetation cover is essential for maintaining ecosystem health, supporting biodiversity, and mitigating climate change impacts.

The study conducted in Kolkata, India, focuses on investigating the impact of various environmental variables on vegetation indices using satellite data from 2003 to 2016. Kolkata, being a densely populated and polluted city in Southeast Asia, experiences significant anthropogenic activities that have led to drastic changes in landscape characteristics and subsequently affect vegetation dynamics. Understanding the long-term variations in weather parameters and their influence on vegetation indices is crucial for sustainable urban environment planning and urban green space management. By analyzing satellite data over a prolonged period, the study seeks to elucidate the relationship between environmental variables and vegetation health in the tropical urban context of Kolkata.

The findings of this study can serve as a valuable reference for researchers, environmental planners, and policymakers involved in sustainable urban development and environmental management. By identifying the key environmental factors influencing vegetation dynamics, stakeholders can make informed decisions regarding land use planning, green space preservation, and mitigation strategies to promote urban biodiversity and enhance the quality of urban environments in a tropical region.

2. Importance of the study location

This study focuses on the spatiotemporal vegetation changes in and around Kolkata, India. Given its geographical location near the Bay of Bengal and within the lower Ganges Delta (Fig. 1), Kolkata experiences a tropical wet and dry climate characterized by a distinct summer monsoon season and significant rainfall, especially during the pre-monsoon period known as *kalbaisakhi*. The city's elevation ranges from 1.5 to 9 m, and its landscape features mangrove forests and tidal flats along the Hooghly River. Considering Kolkata's status as the largest metropolis and a key economic hub in eastern India, understanding the vegetation dynamics in this region is crucial for assessing environmental changes, land use patterns, and their impacts on local ecosystems and livelihoods. By conducting a detailed analysis of satellite-derived vegetation data and considering the unique climatic and geographical characteristics of Kolkata and its surroundings, researchers can uncover valuable insights into the long-term trends and drivers of vegetation dynamics in this region. This information can contribute to informed decision-making processes for urban planning, ecosystem conservation, and climate change adaptation strategies.

3. Dataset

In the present study, monthly data of VIs collected from NASA GIOVANNI have been used in association with meteorological parameters over Kolkata and surrounding locations. The MOD13C2 v. 6 product provides pixel-based VI values of two primary vegetation layers at 1-km spatial resolution. NDVI was derived from the National Oceanic and Atmospheric Administration-Advanced Very High-Resolution

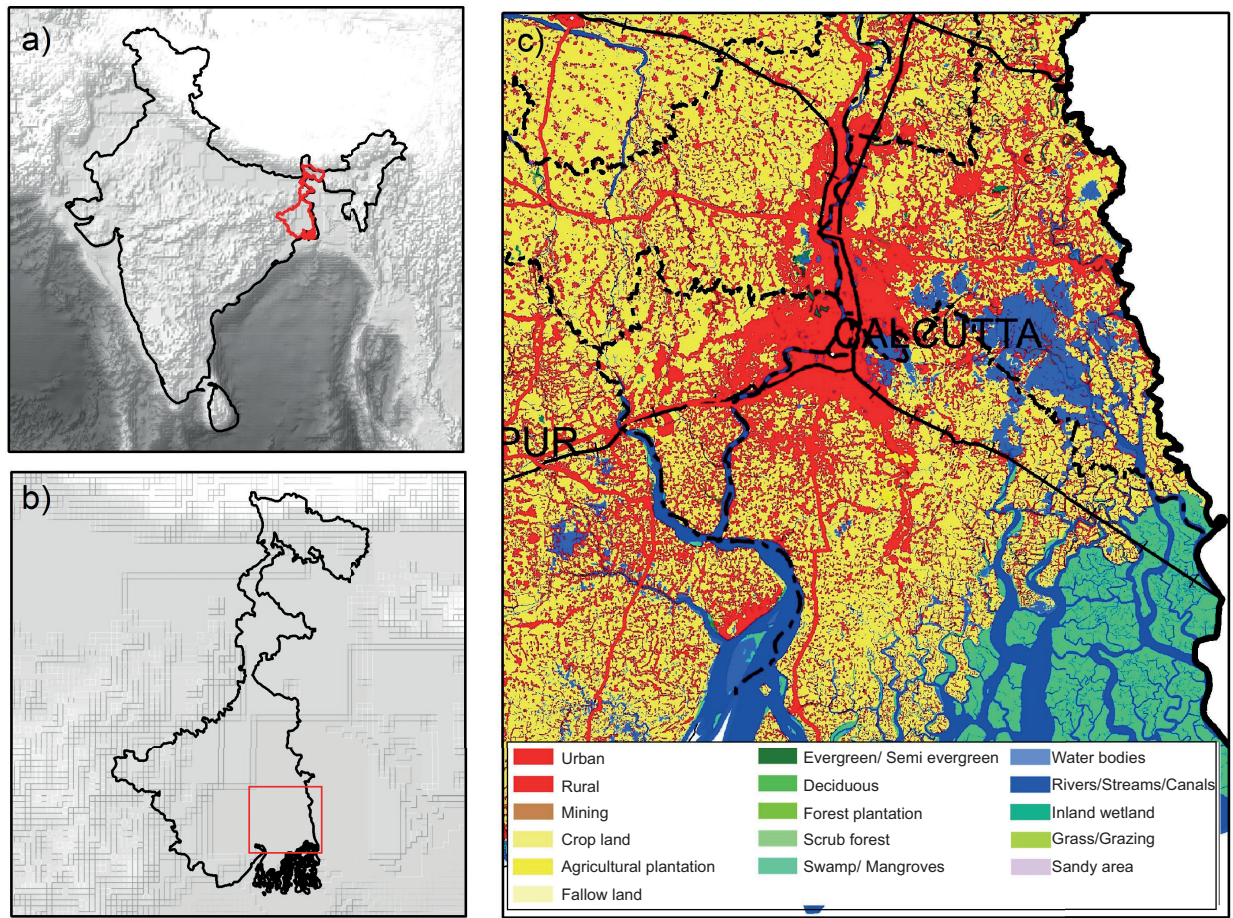


Fig. 1. Location map of the study area.

Radiometer (NOAA-AVHRR). The EVI has better sensitivity over high biomass regions (Didan et al., 2015). From the MOD13C2 v. 6 product, NDVI has been calculated using Eq. (1):

$$NDVI = \frac{(NIR - RED)}{(NIR + RED)} \quad (1)$$

where NIR and RED are the reflectance in the near-infrared and red channels, respectively. The two channels contain more than 90% vegetation information. Monthly precipitation data was obtained from GPM_3IMERGM v. 06. The estimated precipitation from various satellite passive microwave (PMW) sensors consists of GPM constellations and is computed using the Goddard Profiling Algorithm (GPROF2017). This data has been gridded and inter-calibrated to the GPM Combined Ku Radar-Radiometer Algorithm (CORRA) product. This

GPM_3IMERGM provides monthly rainfall with $0.1^\circ \times 0.1^\circ$ spatial resolution (Huffman et al., 2015; McNally et al., 2017, 2019; Skofronick-Jackson et al., 2017; Khan and Gilani, 2021). The average monthly LST values have been taken from the MOD11C3 v. 6 product with 0.05° Climate Modeling Grid (CMG). The CMG granule is a geographic grid that consists of 3600 rows and 7200 columns representing the entire globe. LST values are obtained from the daily average of the corresponding month of MOD11C1 (Wan, 2006; Wan et al., 2015). For SM and ET, Noah 3.6.1 model in the Famine Early Warning Systems Network (FEWS NET) Land Data Assimilation System (FLDAS) has been used. Total ET is related to evaporation and plant transpiration. GPP indicates the amount of carbon compound generated by the photosynthesis process of plants for a given period of time. SIF approximates the GPP. The GPP dataset used

in the present study provides monthly average GPP (carbon $m^{-2} d^{-1}$) with a spatial resolution of 8 km for the period 1982-2016. This GPP data is based on the Monteith light use efficiency (LUE) improved with spatially and temporally optimized FLUXNET tower site data (Madani et al., 2020). This dataset provides global SIF with a $0.05^\circ \times 0.05^\circ$ spatial resolution from August 2002 to December 2018. The Scanning Imaging Absorption Spectrometer for Atmospheric Chartography (SCIAMACHY) and Global Ozone Monitoring Experiment 2 (GOME-2) instruments onboard the MetOp-A satellite are used to retrieve SIF data at a 740 nm wavelength. The dataset can be used for the research on drought, yield estimation, and land degradation evaluation. The details of the datasets are shown in Table I.

4. Methodology

By examining long-term variations of vegetation indices for the period 2003-2016, authors were able to capture changes in vegetation over time. The spatial variation of VIs has been observed to understand the changes. Studying the spatial variation of VIs over three different years, namely, 2003, 2010, and 2016, can provide valuable insights into changes in vegetation cover, health, and distribution over time. Using linear regression curve fitting to analyze inter-annual variability allows a deeper understanding of how vegetation responds to changes in weather conditions such as precipitation, SM, ET, and LST. Investigating monthly variations of these parameters

adds granularity to the analysis, considering the temporal aspect of vegetation dynamics and weather fluctuations. Time average spatial correlation analysis helps to identify patterns across the study area, providing insights into the overall relationship between VIs and weather parameters over the studied period (2003-2016). Furthermore, conducting lag period correlation analysis through the Pearson correlation coefficient allows for exploring the potential delayed effects of weather conditions on vegetation, which can be crucial for understanding ecological processes and predicting future changes. This approach enables the identification of not only the immediate effects but also the delayed impacts of weather conditions on vegetation dynamics. The Pearson correlation coefficient was calculated using Eq. (2):

$$r = \frac{\sum (x_i - \bar{x})(y_i - \bar{y})}{\sqrt{\sum (x_i - \bar{x})^2 \sum (y_i - \bar{y})^2}} \quad (2)$$

where r is the correlation coefficient; x_i and y_i are the values of x and y in the samples, respectively, and \bar{x} and \bar{y} are the mean values of x and y , respectively. The flow chart in Figure 2 shows the methodology.

5. Results and discussion

5.1. Spatial variation

The spatial variation of NDVI, EVI, GPP, and SIF is shown in Figure 3. Different spatial characteristics are observed in different parts of Kolkata and the surrounding region. The characteristics of highly urbanized land use dominate the northern and north-western

Table I. Details of datasets.

Elements	Period	Data source
NDVI	January 2001-December 2022	MOD13V@ v. 6, NASA GIOVANNI
EVI	January 2001-December 2022	MOD13V@ v. 6, NASA GIOVANNI
GPP	January 2001-December 2016	METOP A satellite
SIF	January 2003-December 2018	METOP A satellite
Rainfall	January 2001-September 2021	GPM
LST	July 2002-November 2022	MOD11C3 v. 6
SM	January 2001-November 2022	Noah 3.6.1 FLDAS
ET	January 2001-November 2022	Noah 3.6.1 FLDAS

NDVI: Normalized Difference Vegetation Index; EVI: Enhanced Vegetation Index; GPP: gross primary productivity; SIF: sun-induced chlorophyll fluorescence; LST: land surface temperature; SM: soil moisture; ET: evapotranspiration.

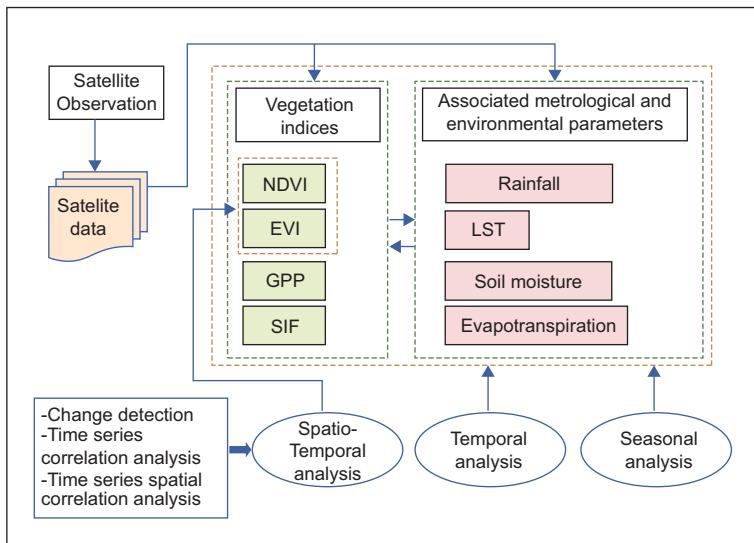


Fig. 2. Flow chart of the research methodology. (NDVI: Normalized Difference Vegetation Index; EVI: Enhanced Vegetation Index; GPP: gross primary productivity; SIF: sun-induced chlorophyll fluorescence; LST: land surface temperature.)

parts of the study area, whereas the eastern part has an abundance of agricultural land use, wetlands, and also a few pockets of urban land use. A dense forest is located in the southeastern part. NDVI, EVI, GPP, and SIF reflect the nature of vegetation and its chlorophyll concentration in a region. Here, the annual average NDVI, EVI, GPP, and SIF of 2003, 2010, and 2016 have been estimated based on available satellite data. In the study area, it is observed that there are spatial differences in the features of NDVI, which are controlled by the nature of land use and land cover characteristics. A lower NDVI value is observed in the highly urbanized lands and wetlands of the Kolkata urban agglomeration, whereas the region with vegetation cover has a higher NDVI. Fig. 3a-c represents the annual average NDVI value for the periods 2003, 2010, and 2016. It has been observed that over that period of time, the nature and concentration of NDVI have increased in the northeastern corner of the study area. A similar trend has been observed in the northwestern part of the study area, where agricultural fields and settlements dominate the land use characteristics. In the south-eastern corner of the study area, no abrupt change is observed from 2003 to 2016. A decreasing trend in NDVI is observed in the eastern part of the study area, where urbanization is growing faster. A similar kind of spatial and temporal change is observed in the case of EVI (Fig 3d-f). GPP indicates the generation and concentration of carbon during the photosynthesis process by plants. There is a spatiotemporal variation in GPP (Fig 3g-i) in the

study area. The higher values of GPP are found in the northeastern, southeastern, and western parts of the study area, whereas the lower values are found in the northwest corner and central to eastern parts. From 2003 to 2016, there is a decreasing trend in GPP in all sectors of the study area. SIF is a functional proxy of terrestrial GPP. The annual average SIF is calculated using METOP A satellite data. In 2003, the higher value of SIF basically concentrated in the north. In the southern, southeastern, and southwestern corners of the study area, a low value of SIF is observed. From 2003 to 2010, a dynamic spatiotemporal change in SIF is observed, whereas there is a sharp increase in SIF in the north, northeast, northwest, and western parts of the study area. However, a sharp decrease in SIF is observed in the east and southeast. From 2010 to 2016, there was a negative change in SIF in all sectors of the study area.

The findings from the analysis of NDVI, EVI, GPP, and SIF data reveal intriguing spatial and temporal patterns in vegetation characteristics and productivity across Kolkata and its surrounding region (Fig 3). Lower NDVI values are observed in highly urbanized and wetland areas, while regions with vegetation cover exhibit higher NDVI values (Fig. 3a-c). Over time, an increase in NDVI concentration is noted in the northeastern and northwestern parts, where agricultural fields and settlements dominate. Conversely, a decreasing trend in NDVI is observed in the eastern part, indicative of rapid urbanization.

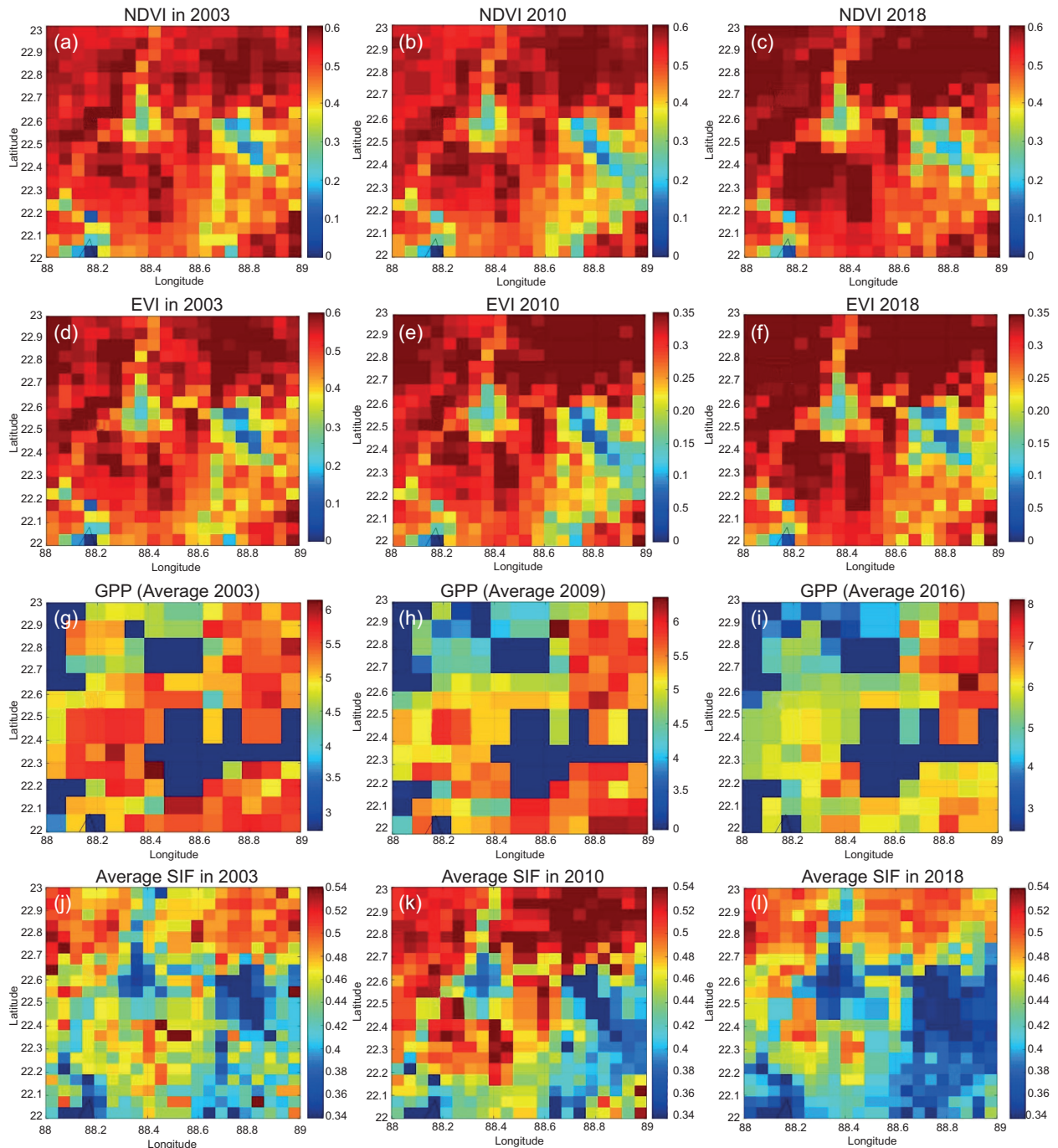


Fig. 3. Spatial variations of (a-c) NDVI for the years 2003, 2010, and 2016, respectively; (d-f) EVI for the years 2003, 2010, and 2016, respectively; (g-i) GPP for the years 2003, 2010, 2016 respectively; and (j-l) SIF for the years 2003, 2010, and 2016, respectively. (NDVI: Normalized Difference Vegetation Index; EVI: Enhanced Vegetation Index; GPP: gross primary productivity; SIF: sun-induced chlorophyll fluorescence).

Similar to NDVI, EVI shows spatial and temporal changes reflecting variations in vegetation greenness. The trends observed in EVI closely mirror those

seen in NDVI, with increasing values in vegetated areas and decreasing values in urbanized regions (Fig. 3d-f). GPP values indicate the generation and

concentration of carbon during photosynthesis by plants. Higher GPP values are concentrated in the northeastern, southeastern, and western parts, while lower values are found in the northwestern and central to eastern parts (Fig. 3g-i). A decreasing trend in GPP is observed across the study area from 2003 to 2016, possibly influenced by various factors including land use changes and climate variability. SIF serves as a functional proxy of terrestrial GPP. Higher SIF values are observed in the north and lower values in the southern, southeastern, and southwestern corners. Dynamic spatiotemporal changes in SIF are noted, with sharp increases in the north, northeast, northwest, and western parts from 2003 to 2010, followed by a negative change in SIF in all areas from 2010

to 2016 (Fig. 3j-l). These observations underscore the complex interplay between land use dynamics, climate variability, and vegetation productivity in the study area. The findings provide valuable insights for ecosystem management, urban planning, and climate change adaptation strategies tailored to the specific characteristics of Kolkata and its surrounding region.

5.2. Interannual variability

The interannual variability of the VI associated with various meteorological parameters, namely precipitation, LST, SM content (0-10 and 10-40 cm), and ET, was investigated for the period 2003-2016 (Fig. 4). The maximum and minimum values are 0.69 and 0.36 for VI, 20.76 and 0.00046 mm for precipitation, 36.64

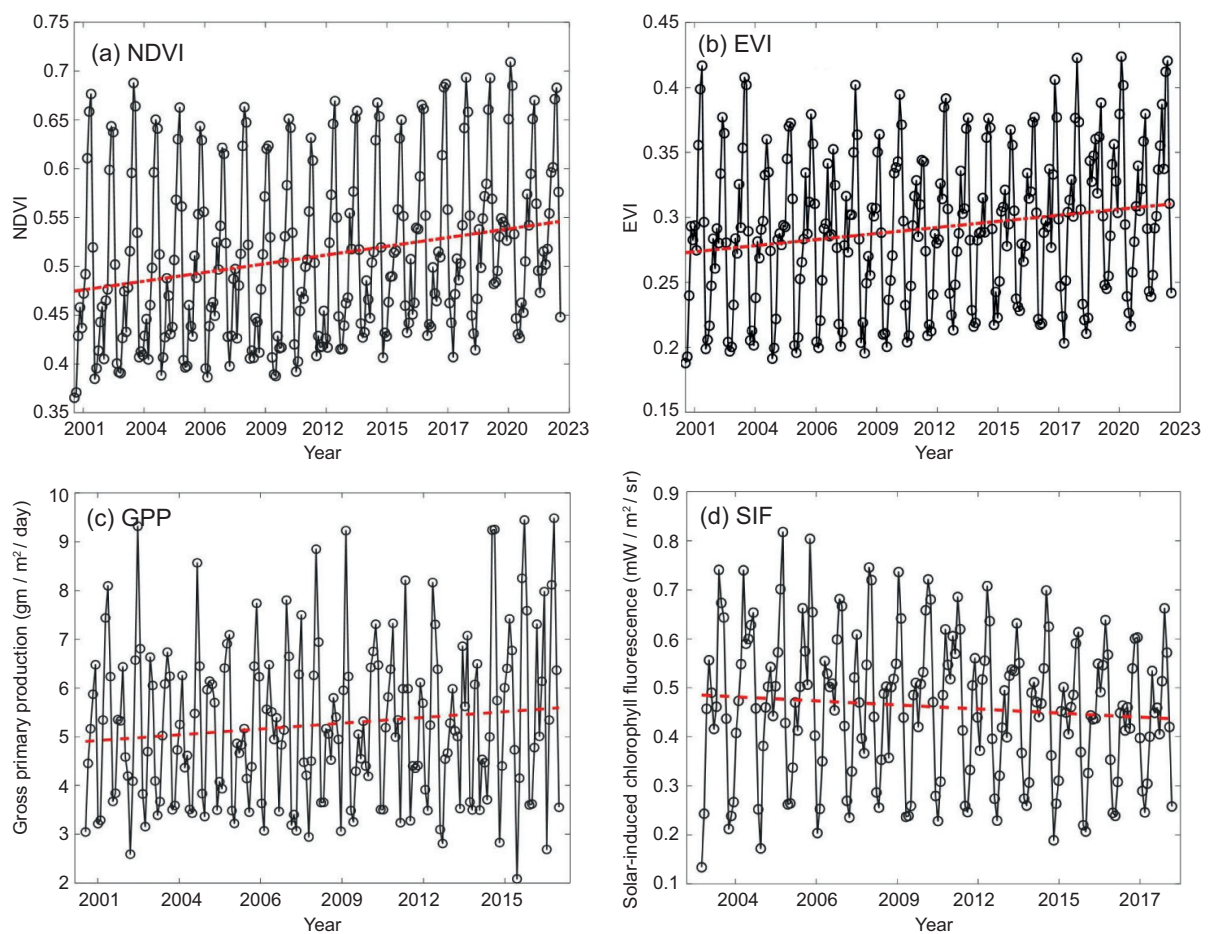


Fig. 4. Yearly variations of (a) NDVI, (b) EVI, (c) GPP, (d) SIF, (e) rainfall (mm), (f) LST (°C), (g) SM (0-10 cm), (h) SM (10-40 cm), (i) ET (kg m⁻² s⁻¹). (NDVI: Normalized Difference Vegetation Index; EVI: Enhanced Vegetation Index; GPP: gross primary productivity; SIF: sun-induced chlorophyll fluorescence; LST: land surface temperature; SM: soil moisture; ET: evapotranspiration). (Continue)

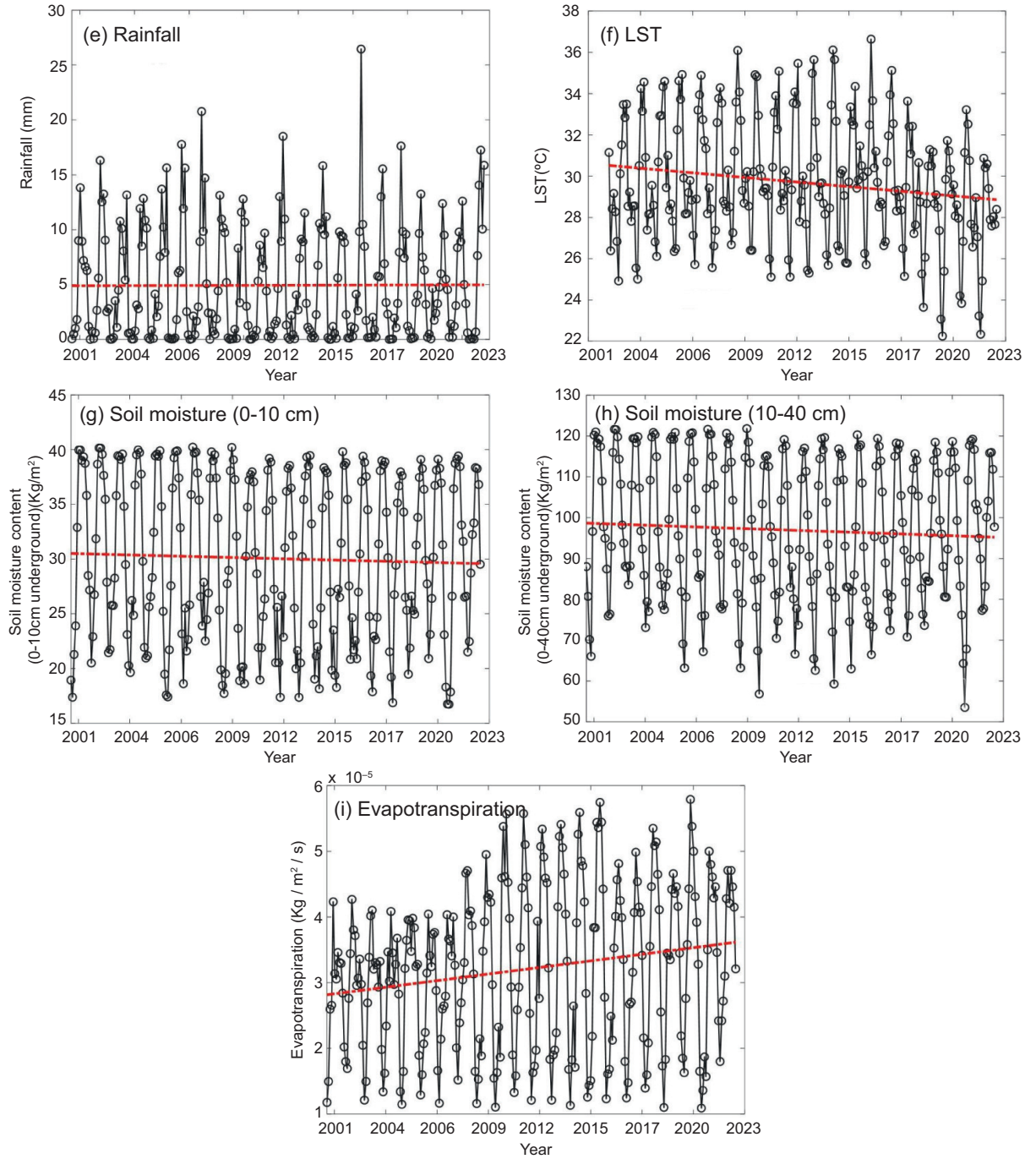


Fig. 4. (Continued) Yearly variations of (a) NDVI, (b) EVI, (c) GPP, (d) SIF, (e) rainfall (mm), (f) LST (°C), (g) SM (0-10 cm), (h) SM (10-40 cm), (i) ET ($\text{kg m}^{-2} \text{s}^{-1}$). (NDVI: Normalized Difference Vegetation Index; EVI: Enhanced Vegetation Index; GPP: gross primary productivity; SIF: sun-induced chlorophyll fluorescence; LST: land surface temperature; SM: soil moisture; ET: evapotranspiration).

and 24.92 °C for LST, 40.23 and 16.88 for SM, and 0.000057 and 0.000011 for ET, respectively. Both precipitation and VI show a good periodic variation

throughout the study period. An increasing trend has been observed with the help of linear regression for VI, ET, LST with a slope of 0.002, 0.0000004 and

0.0007, respectively. A decreasing trend has been observed for precipitation and SM with a slope of 0.001 and 0.009 respectively.

5.3. Monthly variation

The monthly variability of the above parameters is discussed in this section. The monthly average has been calculated for the period 2003-2016 for all parameters and is shown in Fig. 5. It is observed that the average precipitation shows maximum and minimum values in July (36 mm) and December (0.5 mm), respectively. The average values of the maximum and minimum NDVI are observed in September (0.64) and January (0.4), respectively. NDVI values increase from June and decrease after

October (end of the extended monsoon). June to September is considered the grassland growing season and agricultural activities over this location. The maximum and minimum EVI average values were observed in September (0.38) and January (0.21), respectively. The maximum and minimum SM's average values were observed in August (39.12) and February (20.61), respectively. The average value of the maximum and minimum LST were observed in April (34.21 °C) and January (25.82 °C), respectively. Both NDVI and precipitation show a good periodic variation. In the winter season, both NDVI and precipitation show minimum values. It can

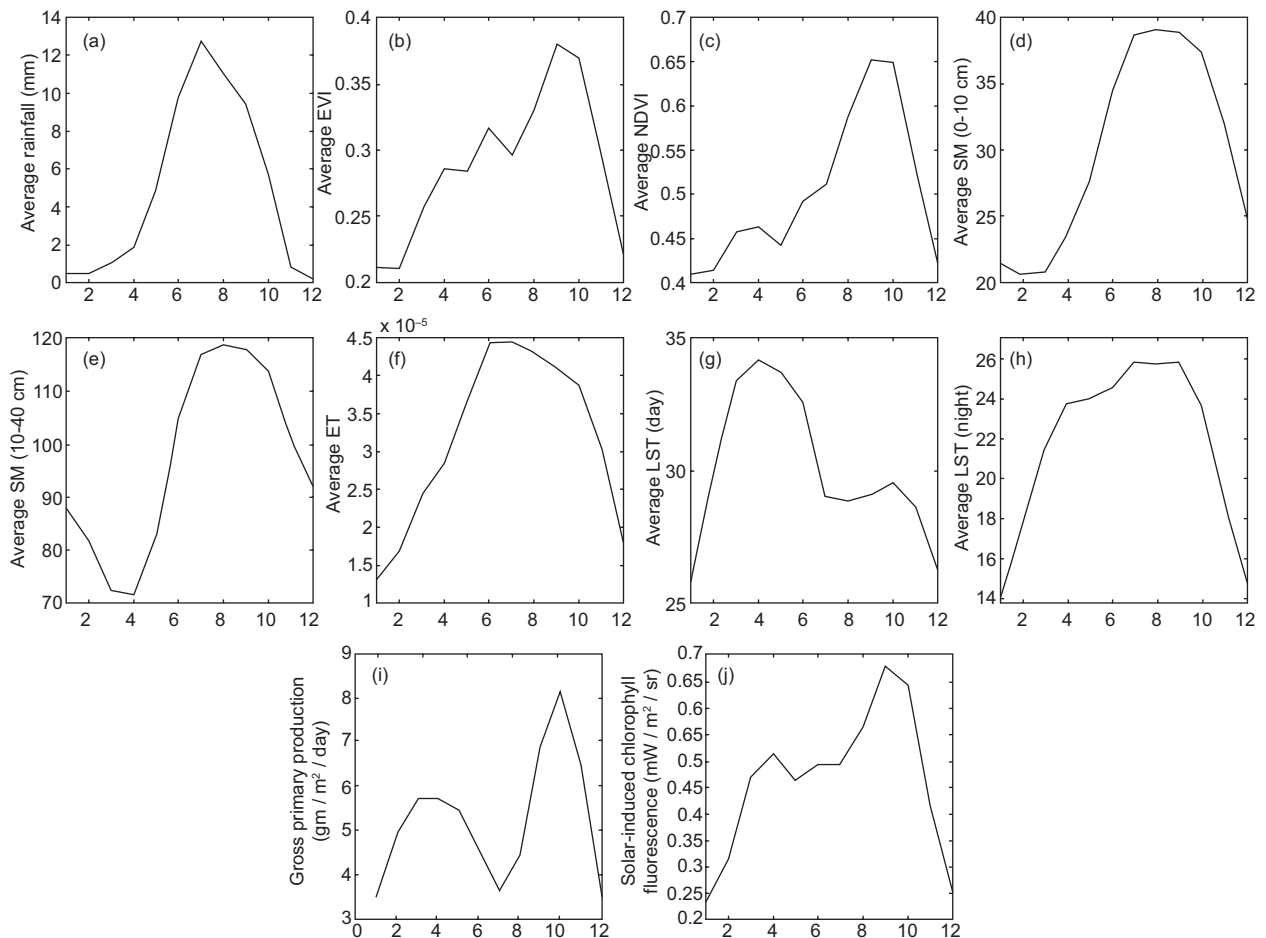


Fig. 5. Monthly variations of average (a) rainfall, (b) EVI, (c) NDVI, (d) SM (0-10 cm), (e) SM (10-40 cm), (f) ET, (g) LST (day), (h) LST (night), (i) GPP, (j) SIF. (EVI: Enhanced Vegetation Index; NDVI: Normalized Difference Vegetation Index; SM: soil moisture; ET: evapotranspiration; LST: land surface temperature; GPP: gross primary productivity; SIF: sun-induced chlorophyll fluorescence.)

be observed that NDVI is related to water availability, as higher NDVI is found during months with higher precipitation. It has also been observed that there is a time lag between high values of precipitation and VI. The time lag between NDVI and other meteorological parameters is discussed in the following section.

5.4. Time average spatial correlation analysis

Spatial analysis consists of locational analysis and the neighboring relationship of phenomena to be studied, whereas time series analysis reflects how observation data changes over a period of time. In this article, spatial time series correlation analysis was carried out to understand the potential interacting pairs of time series across two sequential spatial time series datasets, where a strongly correlated pair of time series indicates that changes of one variable lead to changes in another variable over time. In the present study, spatiotemporal correlation analysis of LST, rainfall, SM, and ET with NDVI and EVI was conducted over the Kolkata conurbation and its surrounding region for 2003-2016. Land use characteristics and their changes have played a dominant role

in determining the nature of land cover in this region, whose northern and northwestern parts are dominated by highly urbanized land use characteristics, whereas the eastern part has an abundance of agricultural land use and wetlands and also a few pockets of urban land use. A dense forest is located in the southeastern part of this area. The spatiotemporal correlation of LST, rainfall, SM, and ET with NDVI is shown in Figure 6a-d. A high to very high positive correlation has been observed near the Kolkata conurbation, which indicates that positive changes of LST lead to changes in NDVI over 2003-2016 (Fig. 6a). In the northeastern and southeastern parts of the study area, a negative correlation was found over this period. This relationship is controlled by the land use and land cover characteristics of the region, which, along with climate and soil, predominately determine the nature of vegetation. Here, the positive correlation exists along the conservation or urban agglomeration of Kolkata and its surrounding areas. These characteristics were observed throughout the mentioned period (2003-2016). In the eastern, northeastern, and southeastern parts of the study area, a negative

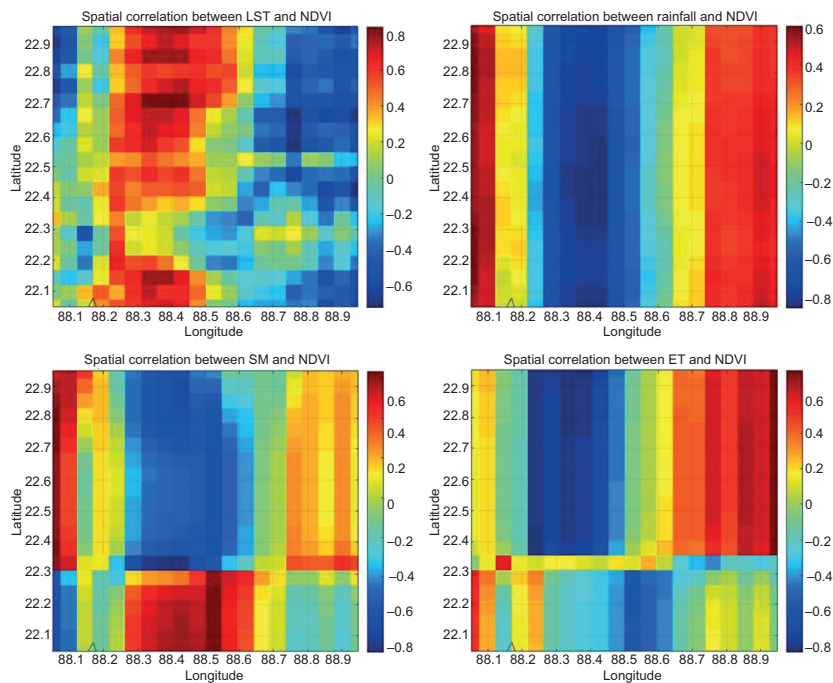


Fig. 6. Time average spatial correlation of NDVI with LST, rainfall, SM, and ET for the period 2003-2016. (NDVI: Normalized Difference Vegetation Index; LST: land surface temperature; SM: soil moisture; ET: evapotranspiration.)

correlation exists between LST and NDVI, where land use characteristics are dominated by agriculture and scattered human settlements.

In general, rainfall and NDVI are positively correlated, but the nature of this relation varies, especially due to its land use characteristics and other climatic and physiographic vegetation processes from 2003 to 2016. The positive correlation between rainfall and NDVI exists along the study area's northeastern, eastern, and southeastern parts; also in the westernmost part of the study area where agricultural land use with high-fertility soil is common. But in the urban agglomeration and its surrounding areas, there is a negative correlation due to the existence of urban land use. Overland water flow is a common phenomenon, and less vegetation concentration has been observed.

The time average spatial correlation of SM and NDVI (shown in Fig. 7 for different parameters) varies spatially. In the study area's eastern, northeastern, southern, and southwestern parts, SM and the nature of NDVI are positively correlated. The existence of agricultural land with fertile alluvial soil

and surface and subsurface water is responsible for such relations. A negative correlation exists between SM and NDVI from 2003 to 2016 in the Kolkata urban agglomeration and its surroundings, where land use is characterized by an overland flow of surface water and lack of tree cover. A negative correlation between SM and NDVI was observed in the southeastern part of the study area, mainly determined by the existence of a mangrove forest and high-salinity soil (Saha et al., 2019).

Cihlar et al. (1991) found a high correlation between NDVI and ET in the growing period. In the study area, a high positive correlation between ET and NDVI was observed in the eastern and northeastern parts, where agricultural practice is performed throughout the year due to the availability of fertile alluvium soil, SM, and irrigation facilities. However, in the urban agglomeration, a negative correlation was observed due to the urban land use and lack of vegetation availability. A negative correlation was also observed in the southern part of the study area. A low-degree positive correlation was found in the southeastern and western parts of the study area due

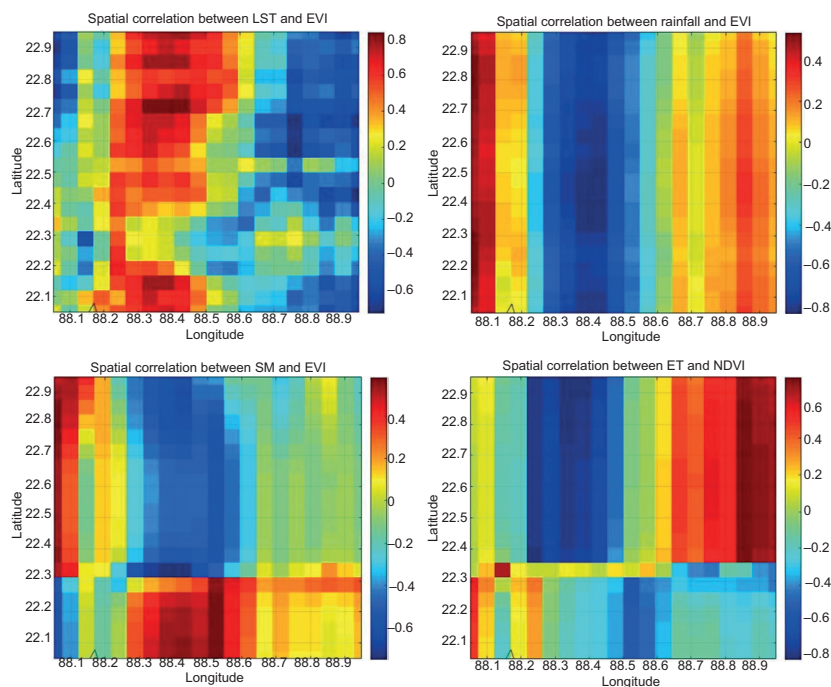


Fig. 7. Time average spatial correlation of EVI with LST, rainfall, SM, and ET for the period 2003-2016. (EVI: Enhanced Vegetation Index; LST: land surface temperature; SM: soil moisture; ET: evapotranspiration.)

to the existence of a vegetation surface. A similar kind of spatial correlation exists between EVI, rainfall, SM, and ET; as a result, it is controlled by land use characteristics and associated pedological and climatic elements. Both positive and negative spatiotemporal correlations have been observed between the meteorological parameters and vegetation index, which are mostly controlled by this location's land use and land cover characteristics.

5.5. Lag period correlation analysis

The lag period correlation analysis between vegetation indices (NDVI, EVI) and meteorological parameters sheds light on the temporal dynamics and interactions between vegetation and environmental factors. In the literature, it has been indicated that the vegetation can respond with a lag in time to meteorological parameters (Sharma et al., 2021; Zhe and Zhang, 2021). The correlation values between NDVI and LST, SM, and precipitation are -0.45 , 0.43 , and 0.34 , respectively, over Gautam Budha Nagar, India (Sharma et al., 2022). The best correlation coefficient (0.66) between NDVI and precipitation has been observed with a one-month lag over South Tibet (Zhe and Zhang, 2021). Due to this fact, the time-lag effects have been investigated in the present study using the correlation analysis between NDVI and other meteorological parameters (0, 1, 2, and 3 months). The maximum correlation with rainfall (0.72), SM (0.83), ET (0.61), and LST (0.83) was observed with a two-month, one-month, two-month, and one-month lag, respectively, for NDVI for the total study period. Regarding EVI, the same time lag was observed with the meteorological parameters but with a reduced correlation coefficient value. It may be because EVI mainly represents high biomass regions. The correlation coefficients of EVI with rainfall, SM, ET, and LST are 0.52 (two-months lag), 0.68 (one-month lag), 0.49 (two-months lag), and -0.72 (one-month lag), respectively. The variation of meteorological parameters with NDVI and EVI for the best correlation time month is shown in Figures 8 and 9, respectively. The variation of meteorological parameters with GPP and SIF for the best correlation time month is shown in Figures 10 and 11, respectively. The variation of meteorological parameters with GPP and SIF for the best correlation time month is shown in

Figures 10 and 11, respectively. A significant positive correlation was observed between NDVI and precipitation for a two-month lag period. Vegetation primarily depends on the natural water supply, which in turn depends on precipitation. Vegetation shows a slow rate of response to rainfall. The NDVI-precipitation correlation further relies on other factors, such as land cover, temperature, SM, and others (Xiong et al., 2003; Wang et al., 2013; Huang et al., 2017). The sensitivity of vegetation is also dependent on SM and ET. SM plays a crucial role in controlling the life span of plants, which affects the evaporation rate and ET of leaves (Xiong et al., 2003; Huang et al., 2017). A positive correlation has been observed between NDVI and ET, as NDVI is directly proportional to vaporized water entering the atmosphere. A negative correlation has been observed between NDVI and LST over this region, which can be triggered by the topography of a particular region (Peng et al., 2020). LST in the urban location has an inverse relation with vegetation due to the effect of land surface materials (Yue et al., 2007). The correlation analysis of VI with different meteorological parameters for different time lag periods is shown in Table II.

6. Conclusion

This study investigates the long-term characteristics of VIs over Kolkata and its surroundings from 2003 to 2016, using satellite-based observations. NDVI, EVI, GPP, and SIF are analyzed, along with their relation to meteorological parameters such as precipitation, SM, ET, and LST. The following are our main observations:

1. Interannual variability is observed for VI and meteorological parameters, with the highest and lowest VI values occurring in September and January, respectively. There is a notable increasing trend in VI, ET, and LST, while precipitation and SM show decreasing trends over the study period.
2. NDVI reflects water availability, showing higher values during months with more rainfall. There is a time lag between peak precipitation and maximum vegetation, typically observed in August-September, coinciding with the monsoon period.

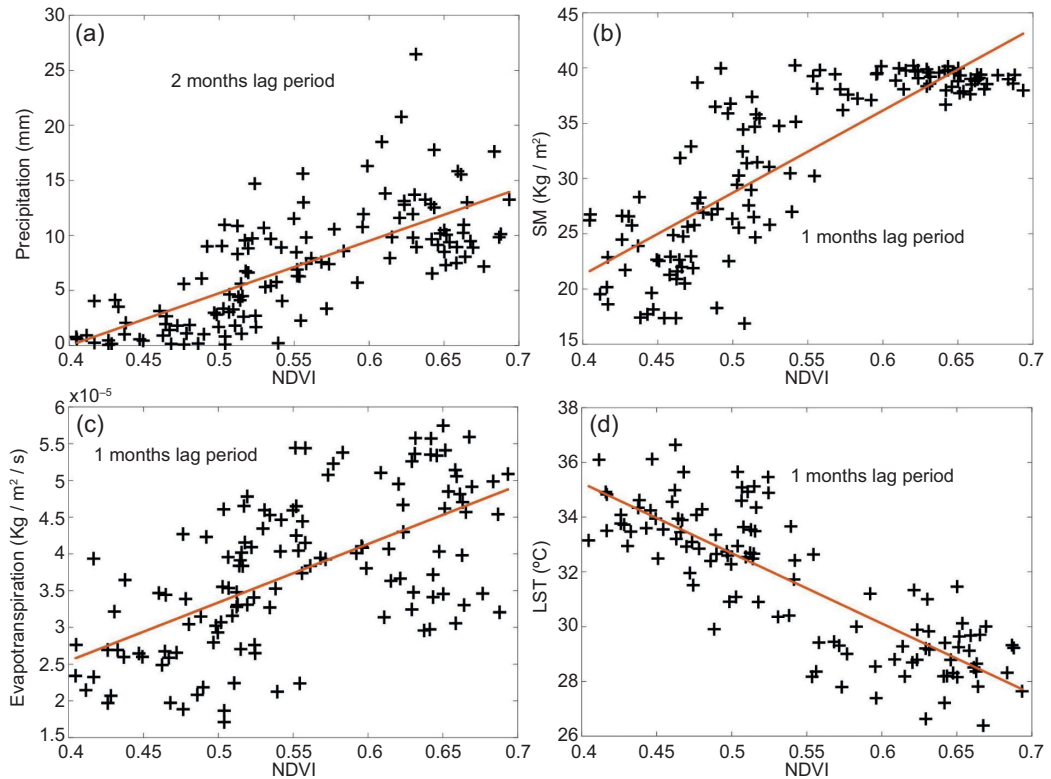


Fig. 8. Best correlation for different lag months of NDVI with (a) precipitation, (b) SM, (c) ET, and (d) LST. (NDVI: Normalized Difference Vegetation Index; SM: soil moisture; ET: evapotranspiration; LST: land surface temperature)

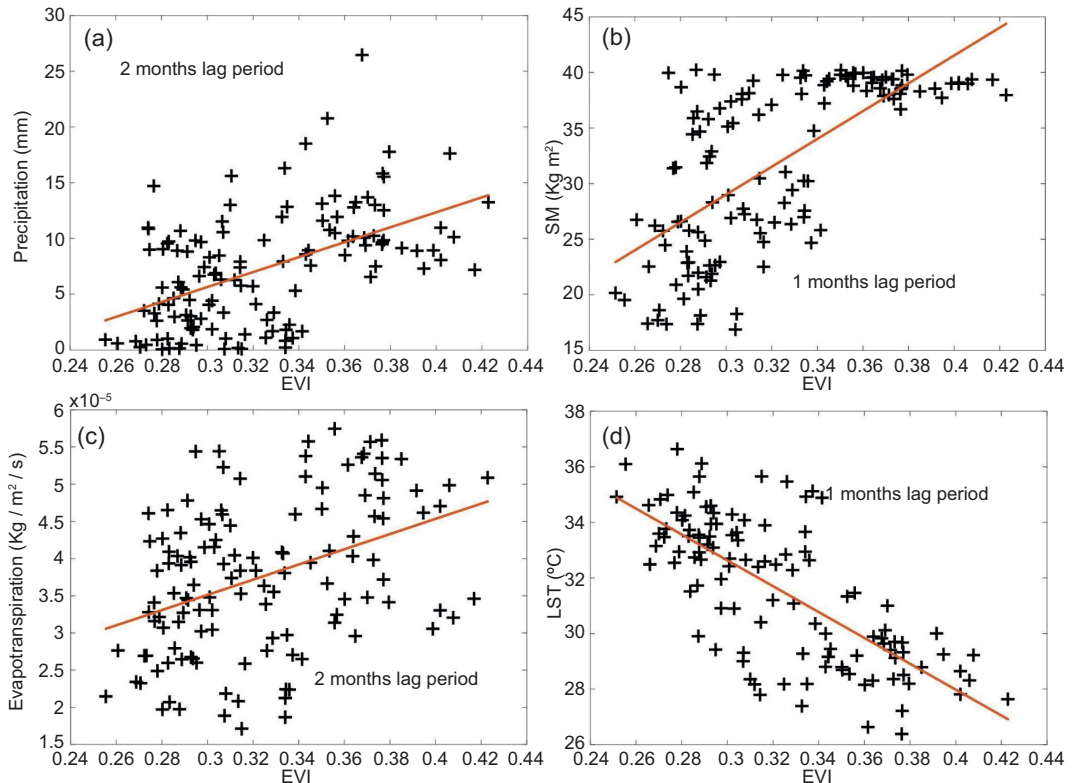


Fig. 9. Best correlation for different lag months of EVI with (a) precipitation, (b) SM, (c) ET, and (d) LST. (EVI: Enhanced Vegetation Index; SM: soil moisture; ET: evapotranspiration; LST: land surface temperature).

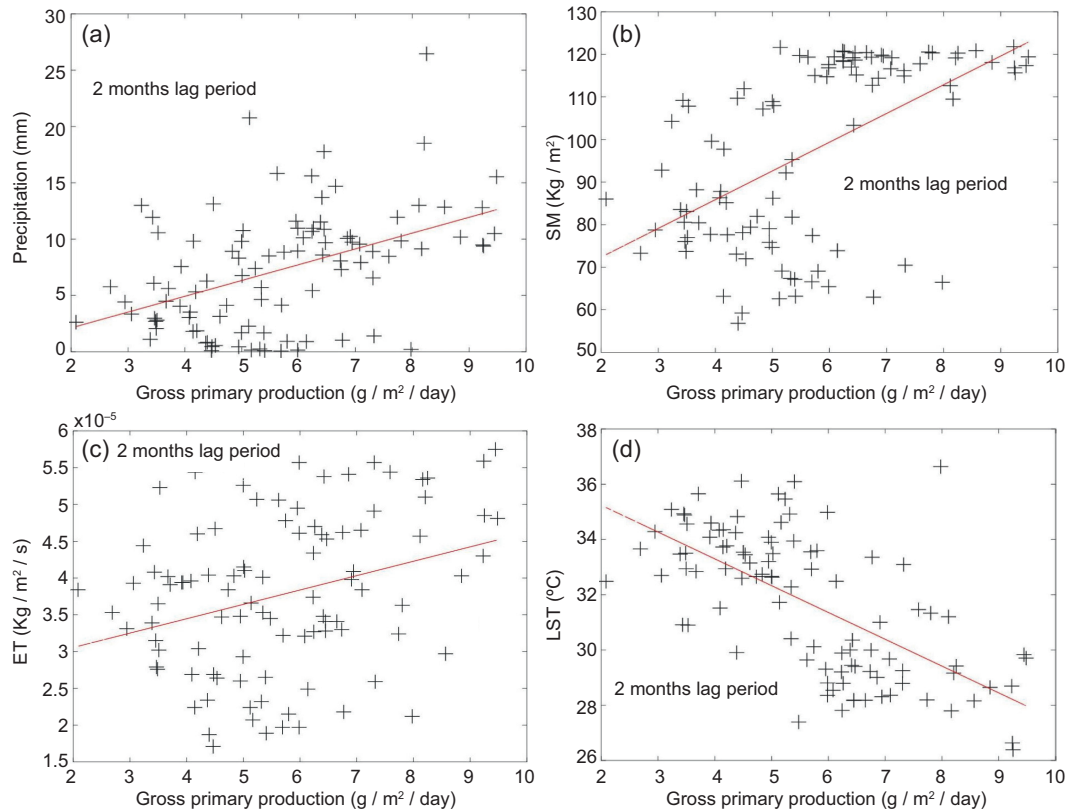


Fig. 10. Best correlation for different lag months of GPP with (a) precipitation, (b) SM, (c) ET, and (d) LST. (GPP: gross primary productivity; SM: soil moisture; ET: evapotranspiration; LST: land surface temperature.)

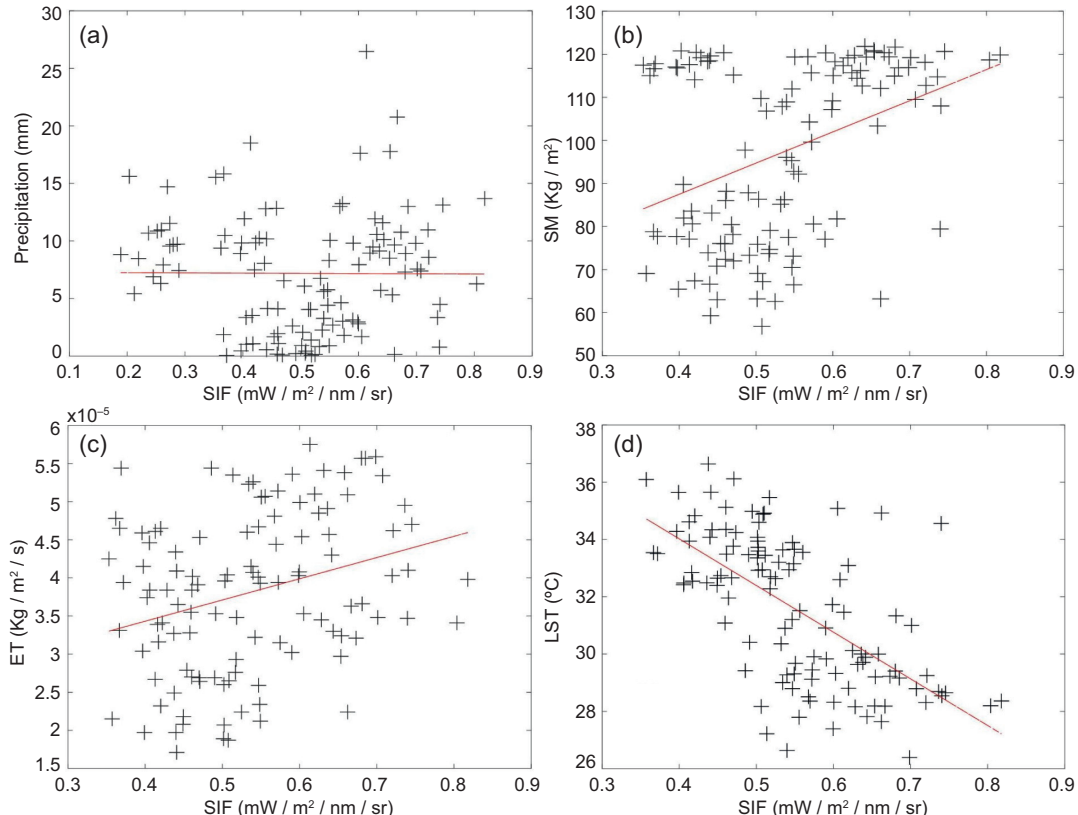


Fig 11. Best correlation for different lag months of SIF with (a) precipitation, (b) SM, (c) ET, and (d) LST. (SIF: sun-induced chlorophyll fluorescence; SM: soil moisture; ET: evapotranspiration; LST: land surface temperature.)

Table II. Correlation analysis of VI with different meteorological parameters for different time lag periods.

Elements	0 month (March–September)	1 month (April–October)	2 months (May–November)
NDVI			
Rainfall	0.45	0.62	0.72
Soil moisture (0-10 cm)	0.70	0.83	0.77
Soil moisture (10-40 cm)	0.72	0.85	0.76
Evapotranspiration	0.42	0.54	0.61
Land surface temperature	-0.78	-0.83	-0.64
EVI			
Rainfall	0.38	0.40	0.52
Soil moisture (0-10 cm)	0.67	0.68	0.52
Soil moisture (10-40 cm)	0.44	0.46	0.26
Evapotranspiration	0.40	0.43	0.49
Land surface temperature	-0.60	-0.72	-0.47
GPP			
Rainfall	0.19	0.21	0.46
Soil moisture (0-10 cm)	0.12	0.19	0.51
Soil moisture (10-40 cm)	0.12	0.21	0.55
Evapotranspiration	-0.09	0.03	0.32
Land surface temperature	0.09	-0.32	-0.64
SIF			
Rainfall	0.22	0.41	0.43
Soil moisture (0-10 cm)	0.46	0.59	0.4
Soil moisture (10-40 cm)	0.47	0.62	0.38
Evapotranspiration	0.15	0.25	0.29
Land surface temperature	-0.49	-0.63	-0.33

3. Spatial variations in NDVI are linked to land use characteristics. Areas dominated by agriculture show increased NDVI, while regions undergoing urbanization exhibit decreasing trends. Land use, climate, and soil properties influence vegetation dynamics.
4. Time lag effects are explored through correlation analysis between NDVI and meteorological parameters, revealing significant correlations within one to two-month periods. NDVI shows positive correlations with precipitation, SM, and ET, while an inverse correlation is observed with LST, influenced by land surface materials and topography.

Overall, the study provides insights into the long-term spatiotemporal dynamics of VIs and their relationship

with meteorological parameters in a tropical urban area, aiding in understanding ecosystem responses to environmental changes. Expanding the study beyond Kolkata to other metropolitan cities in India to observe vegetation cover dynamics in relation to meteorological parameters is a commendable initiative. By broadening the scope of the study, researchers can gain insights into the spatiotemporal characteristics of vegetation indices across different urban agglomerations in India and assess the influence of meteorological factors on vegetation health and dynamics. This extended research effort has the potential to contribute significantly to our understanding of urban vegetation dynamics and their relationship with meteorological parameters on a broader scale. By comparing vegetation responses across multiple

metropolitan areas, researchers can identify common patterns, drivers, and trends, facilitating the development of a comprehensive model describing how vegetation changes with meteorological effects over the long term in Indian urban contexts. Such a model could have practical implications for urban planning, environmental management, and climate resilience strategies in Indian metropolitan cities. By integrating satellite observations, meteorological data, and vegetation indices, policymakers and urban planners can make informed decisions to promote sustainable urban development, enhance green infrastructure, and mitigate the impacts of climate change on urban ecosystems and human well-being. Overall, the planned extension of the study to other metropolitan cities in India holds great promise for advancing our knowledge of urban vegetation dynamics and informing evidence-based policies and practices for sustainable urban development.

References

Adegoke JO, Andrew MC. 2002. Relations between soil moisture and satellite vegetation indices in the U.S. Corn Belt. *Journal of Hydrometeorology* 3: 395-405. [http://doi.org/10.1175/1525-7541\(2002\)003%3C0395:RBSMAS%3E2.0.CO;2](http://doi.org/10.1175/1525-7541(2002)003%3C0395:RBSMAS%3E2.0.CO;2)

Akram R, Amanet K, Iqbal J, Fatima M, Mubeen M, Hussain S, Ali M, Nasim W, Ahmad A, Farid HU, El Sabagh A, Fahad S. 2022. Climate change, insects and global food production. In: *Climate change ecosystem: Challenges to sustainable development* (Fahad S, Adnan M, Saud S, Nie L, Eds.). CRC Press, Boca Raton, 47-60. <http://doi.org/10.1201/9781003286400-3>

Akram R, Turan V, Hammad HM, Ahmad S, Hussain S, Hasnain A, Maqbool MM, Rehmani MIA, Rasool A, Masood N, Mahmood F, Mubeen M, Sultana SR, Fahad S, Amanet K, Saleem M, Abbas Y, Akhtar HM, Hussain S, Wassem R, Amin A, Zahoor SA, Sami ul Din M, Nasim W. 2018. Fate of organic and inorganic pollutants in paddy soils. In: *Environmental pollution of paddy soils* (Hashmi MZ, Varma A, Eds.). Soil Biology 53. Springer, Cham. https://doi.org/10.1007/978-3-319-93671-0_13

Ali M, Mubeen M, Hussain N, Wajid A, Farid HU, Awais M, Hussain S, Akram W, Amin A, Akram R, Imran M, Ali A, Nasim W. 2019. Role of ICT in crop management. In: *Agronomic crops*. Vol. 2: Management practices (Hasanuzzaman M, Ed.). Springer, Singapore, 637-652. https://doi.org/10.1007/978-981-32-9783-8_28

Amin A, Nasim W, Mubeen M, Nadeem M, Ali L, Hammad HM, Sultana SR, Jabran K, Rehman MHur, Ahmad S, Awais M, Rasool A, Fahad S, Saud S, Shah AN, Ihsan Z, Bajwa AA, Hakeem KR, Ameen A, Amanullah, Rehman HU, Alghabar F, Jatoi GH, Akram M, Khan A, Islam F, Ata-Ul-Karim ST, Rehmani MIA, Hussain S, Rezaq M, Fathi A. 2017. Optimizing the phosphorus use in cotton by using CSM-CROPGRO-cotton model for semi-arid climate of Vehari-Punjab, Pakistan. *Environmental Science and Pollution Research* 24: 5811-5823. <https://doi.org/10.1007/s11356-016-8311-8>

Aslam B, Maqsoom A, Khalid N, Ullah F, Sepasgozar S. 2021. Urban overheating assessment through prediction of surface temperatures: a case study of Karachi, Pakistan. *ISPRS International Journal of Geo-Information* 10: 539. <https://doi.org/10.3390/ijgi10080539>

Baqi MF, Lu L, Chen F, Nawaz-ul-Huda S, Pan L, Tariq A, Qureshi S, Li B, Li Q. 2022. Characterizing spatio-temporal variations in the urban thermal environment related to land cover changes in Karachi, Pakistan, from 2000 to 2020. *Remote Sensing* 14: 2164. <https://doi.org/10.3390/rs14092164>

Basistha A, Arya DS, Goel NK. 2009. Analysis of historical changes in rainfall in the Indian Himalayas. *International Journal of Climatology: A Journal of the Royal Meteorological Society* 29: 555-572. <https://doi.org/10.1002/joc.1706>

Bhandaria AK, Kumara A, Singh GK. 2012. Feature extraction using Normalized Difference Vegetation Index (NDVI): A case study of Jabalpur City. *Procedia Technology* 6: 612-621. <https://doi.org/10.1016/j.protcy.2012.10.074>

Cao Z, Li Y, Liu Y, Chen Y, Wang Y. 2018. When and where did the Loess Plateau turn “green”? Analysis of the tendency and breakpoints of the normalized difference vegetation index. *Land Degradation & Development* 29: 162-175. <https://doi.org/10.1002/lde.2852>

Chandra N, Singh G, Rai ID, Mishra AP, Kazmi MY, Pandey A, Jalal JS, Costache R, Almohamad H, al-Mutiry M, Abdo HG. 2023. Predicting distribution and range dynamics of three threatened cypripedium species under climate change scenario in Western Himalaya. *Forests* 14: 633. <https://doi.org/10.3390/f14030633>

Choubin B, Solaimani K, Roshan MH, Malekian A. 2017. Watershed classification by remote sensing indices: A fuzzy c-means clustering approach. *Journal of Mountain Science* 14: 2053-2063. <https://doi.org/10.1007/s11629-017-4357-4>

Cihlar J, St Laurent L, Dyer JA. 1991. Relation between the normalized difference vegetation index and ecological variables. *Remote sensing of Environment* 35: 279-298. [https://doi.org/10.1016/0034-4257\(91\)90018-2](https://doi.org/10.1016/0034-4257(91)90018-2)

Cleland EE, Chiariello NR, Loarie SR, Mooney HA, Field CB. 2006. Diverse responses of phenology to global changes in a grassland ecosystem. *Proceedings of the National Academy of Sciences* 103: 13740-13744. <https://doi.org/10.1073/pnas.0600815103>

Dagnachew M, Kebede A, Moges A, Abebe A. 2020. Effects of climate variability on Normalized Difference Vegetation Index (NDVI) in the Gojeb River catchment, Omo-Gibe Basin, Ethiopia. *Advances in Meteorology*: 8263246. <https://doi.org/10.1155/2020/8263246>

De A, Shreya S, Sarkar N, Maitra A. 2023. Time series trend analysis of rainfall and temperature over Kolkata and surrounding region. *Atmósfera* 37: 71-84. <https://doi.org/10.20937/ATM.53059>

Demirel H, Ozcinar C, Anbarjafari G. 2010. Satellite image contrast enhancement using discrete wavelet transform and singular value decomposition. *IEEE Geoscience Remote Sensing Letters* 7: 333-337. <https://doi.org/10.1109/LGRS.2009.2034873>

Didan K, Barreto Muñoz A, Solano R, Huete A. 2015. MODIS vegetation index user's guide (MOD13 series) version 3.00. *Vegetation Index and Phenology Lab*, University of Arizona.

Din MSU, Mubeen M, Hussain S, Ahmad A, Hussain N, Ali MA, El Sabagh A, Elsabagh M, Shah GM, Qaisrani SA, Tahir M, Javeed HMR, Anwar-ul-Haq M, Ali M, Nasim W. 2022. World nations priorities on climate change and food security. In: *Building climate resilience in agriculture* (Jatoi WN, Mubeen M, Ahmad A, Cheema MA, Lin Z, Hashmi MZ, eds.). Springer, Cham, 365-384. https://doi.org/10.1007/978-3-030-79408-8_22

Duhan D, Pandey A. 2013. Statistical analysis of long term spatial and temporal trends of precipitation during 1901-2002 at Madhya Pradesh, India. *Atmospheric Research* 122: 136-149. <http://doi.org/10.1016/j.atmosres.2012.10.010>

Dutta D, Kundu A, Patel NR, Saha SK, Siddiqui AR. 2015. Assessment of agricultural drought in Rajasthan (India) using remote sensing derived Vegetation Condition Index (VCI) and Standardized Precipitation Index (SPI). *The Egyptian Journal of Remote Sensing and Space Science* 18: 53-63. <https://doi.org/10.1016/j.ejrs.2015.03.006>

Eastman JR, Sangermano F, Machado EA, Rogan J, Anyamba A. 2013. Global trends in seasonality of normalized difference vegetation index (NDVI), 1982-2011. *Remote Sensing* 5: 4799-4818. <https://doi.org/10.3390/rs5104799>

Fahad S, Bajwa AA, Nazir U, Anjum SA, Farooq A, Zohaib A, Sadia S, Nasim W, Adkins S, Saud S, Ihsan MZ, Alharby H, Wu Chao, Wang D, Huang J. 2017. Crop production under drought and heat stress: Plant responses and management options. *Frontiers in Plant Science* 8: 1147. <https://doi.org/10.3389/fpls.2017.01147>

Farrar TJ, Nicholson SE, Lare AR. 1994. The influence of soil type on the relationships between NDVI, rainfall, and soil moisture in semiarid Botswana. II. NDVI response to soil moisture. *Remote Sensing of Environment* 50: 121-133. [https://doi.org/10.1016/0034-4257\(94\)90039-6](https://doi.org/10.1016/0034-4257(94)90039-6)

Feizizadeh B, Blaschke T, Nazmfar H, Akbari E, Kohbanani HR. 2013. Monitoring land surface temperature relationship to land use/land cover from satellite imagery in Maraqeh County, Iran. *Journal of Environmental Planning and Management* 56: 1290-1315. <https://doi.org/10.1080/09640568.2012.717888>

Gao SG, Zhu ZL, Liu SM, Jin R, Yang GC, Tan L. 2014. Estimating the spatial distribution of soil moisture based on Bayesian maximum entropy method with auxiliary data from remote sensing. *International Journal of Applied Earth Observation and Geoinformation* 32: 54-66. <https://doi.org/10.1016/j.jag.2014.03.003>

Gautam S, Brema J, Dhasarathan R. 2020. Spatio-temporal estimates of solid waste disposal in an urban city of India: A remote sensing and GIS approach. *Environmental Technology & Innovation* 18: 100650. <https://doi.org/10.1016/j.eti.2020.100650>

Gheorghe IF, Ion B. 2011. The effects of air pollutants on vegetation and the role of vegetation in reducing atmospheric pollution. In: *The impact of air pollution on health, economy, environment and agricultural sources* (Khalla M, Ed.). IntechOpen, 241-280. <https://doi.org/10.5772/17660>

Gu Y, Hunt E, Wardlow B, Basara JB, Brown JF, Verdin JP. 2008. Evaluation of MODIS NDVI and NDWI for

vegetation drought monitoring using Oklahoma Mesonet soil moisture data. *Geophysical Research Letters* 35. <https://doi.org/10.1029/2008GL035772>

Hassan QK, Ejiaha IR, Ahmed MR, Gupta A, Rangelova E, Dewan A. 2021. Remote sensing of local warming trend in Alberta, Canada during 2001-2020, and Its relationship with large-scale atmospheric circulations. *Remote Sensing* 13: 3441. <https://doi.org/10.3390/rs13173441>

Hateffard F, Mohammed S, Alsafadi K, Enaruvbe GO, Heidari A, Abdo HG, Rodrigo-Comino J. 2021. CMIP5 climate projections and RUSLE-based soil erosion assessment in the central part of Iran. *Scientific Reports* 11: 7273. <https://doi.org/10.1038/s41598-021-86618-z>

Huang S, Huang Q, Leng G, Zhao M, Meng E. 2017. Variations in annual water-energy balance and their correlations with vegetation and soil moisture dynamics: A case study in the Wei River Basin, China. *Journal of Hydrology* 546: 515-525. <https://doi.org/10.1016/j.jhydrol.2016.12.060>

Huete A, Didan K, Miura T, Rodriguez EP, Gao X, Ferreira LG. 2002. Overview of the radiometric and biophysical performance of the MODIS vegetation indices. *Remote Sensing of Environment* 83: 195-213. [https://doi.org/10.1016/S0034-4257\(02\)00096-2](https://doi.org/10.1016/S0034-4257(02)00096-2)

Huffman GJ, Bolvin DT, Nelkin EJ, Tan J. 2015. Integrated Multi-satellitE Retrievals for GPM (IMERG) technical documentation. NASA/GSFC Code 612(47).

Hussain S, Ahmad A, Wajid A, Khaliq T, Hussain N, Mubeen M, Farid HU, Imran M, Hammad HM, Awais M, Ali A, Aslam M, Amin A, Amanet K, Nasim W. 2020a. Irrigation scheduling for cotton cultivation. In: Cotton production and uses: Agronomy, crop protection, and postharvest technologies (Ahmad S, Hasanuzzaman M, Eds.). Springer, Singapore, 59-80. https://doi.org/10.1007/978-981-15-1472-2_5

Hussain S, Mubeen M, Ahmad A, Akram W, Hammad HM, Ali M, Masoon N, Amin A, Farid HU, Sultana SR, Fahad S, Wang D, Nasim W. 2020b. Using GIS tools to detect the land use/land cover changes during forty years in Lodhran District of Pakistan. *Environmental Science and Pollution Research* 27: 39676-39692. <https://doi.org/10.1007/s11356-019-06072-3>

Hussain S, Mubeen M, Ahmad A, Fahad S, Nasim W, Hammad HM, Shah GM, Murtaza B, Tahir M, Parveen S. 2023a. Using space-time scan statistic for studying the effects of COVID-19 in Punjab, Pakistan: A guideline for policy measures in regional agriculture. *Environmental Science and Pollution Research* 30: 42495-42508. <https://doi.org/10.1007/s11356-021-17433-2>

Hussain S, Raza A, Abdo HG, Mubeen M, Tariq A, Nasim W, Majid M, Almohamad H, al Dughairi AA. 2023b. Relation of land surface temperature with different vegetation indices using multi-temporal remote sensing data in Sahiwal region, Pakistan. *Geoscience Letters* 10: 33. <https://doi.org/10.1186/s40562-023-00287-6>

Ichii K, Kawabata A, Yamaguchi Y. 2002. Global correlation analysis for NDVI and climatic variables and NDVI trends: 1982-1990. *International Journal of Remote Sensing* 23: 3873-3878. <https://doi.org/10.1080/01431160110119416>

Karuppasamy MB, Natesan U, Karuppannan S, Chandrasekaran LN, Hussain S, Almohamad H, Dughairi AAA, Al-Mutiry M, Alkayyadi I, Abdo HG. 2022. Multivariate urban air quality assessment of indoor and outdoor environments at Chennai Metropolis in South India. *Atmosphere* 13: 1627. <https://doi.org/10.3390/atmos13101627>

Khan R, Gilani H. 2021. Global drought monitoring with big geospatial datasets using Google Earth Engine. *Environmental Science and Pollution Research* 28: 17244-17264. <https://doi.org/10.1007/s11356-020-12023-0>

Lakshmi Kumar TV, Barbosa HA. 2012. Anomalous changes in summer monsoon rainfall and crop yields over India. *Disaster Advances* 5: 52-62.

Kundu A, Dutta D. 2011. Monitoring desertification risk through climate change and human interference using remote sensing and GIS techniques. *International Journal of Geomatics and Geoscience* 2: 21-33.

Kundu A, Patel NR, Saha SK, Dutta D. 2017. Desertification in western Rajasthan (India): An assessment using remote sensing derived rain-use efficiency and residual trend methods. *Natural Hazard* 86: 297-313. <https://doi.org/10.1007/s11069-016-2689-y>

Li W, Migliavacca M, Forkel M, Denissen JMC, Reichstein M, Yang H, Duveiller G, Weber U, Orth R. 2022. Widespread increasing vegetation sensitivity to soil moisture. *Nature Communications* 13: 3959. <https://doi.org/10.1038/s41467-022-31667-9>

Liu HQ, Huete A. 1995. A feedback based modification of the NDVI to minimize canopy background and atmospheric noise. *IEEE Transactions on Geoscience and Remote Sensing* 33: 457-465. <https://doi.org/10.1109/TGRS.1995.8746027>

Lu L, Kuenzer C, Wang C, Guo H, Li Q. 2015. Evaluation of three MODIS-derived vegetation index time series for dryland vegetation dynamics monitoring. *Remote Sensing* 7: 7597-7614. <https://doi.org/10.3390/rs70607597>

Madani N, Parazoo NC. 2020. Global monthly GPP from an improved light use efficiency model, 1982-2016. Oak Ridge National Laboratory Distributed Active Archive Center (ORNL DAAC). Oak Ridge, Tennessee, USA. <https://doi.org/10.3334/ORN-LDAAC/1789>

Mallick J, Singh CK, Shashtri S, Rahman A, Mukherjee S. 2012. Land surface emissivity retrieval based on moisture index from LANDSAT TM satellite data over heterogeneous surfaces of Delhi city. *International Journal of Applied Earth Observation and Geoinformation* 19 (2012): 348-358. <https://doi.org/10.1016/j.jag.2012.06.002>

Masood N, Akram R, Fatima M, Mubeen M, Hussain S, Shakeel M, Khan N, Adnan M, Wahid A, Shah AN, Ihsan MZ, Rasool A, Ullah K, Awais M, Abbas M, Hussain D, Shahzad K, Bibi F, Ahmad I, Khan I, Hussain K, Nasim W. 2022. Insect pest management under climate change. In: *Building climate resilience in agriculture: Theory, practice and future perspective* (Jatoi WN, Mubeen M, Ahmad A, Cheema MA, Lin Z, Hashmi MZ, Eds.). Springer, Cham, 225-237. https://doi.org/10.1007/978-3-030-79408-8_15

Matsushita B, Yang W, Chen J, Onda Y, Qiu G. 2007. Sensitivity of the Enhanced Vegetation Index (EVI) and Normalized Difference Vegetation Index (NDVI) to topographic effects: A case study in high-density cypress forest. *Sensors* 7: 2636-2651. <https://doi.org/10.3390/s7112636>

McNally A, Arsenault K, Kumar S, Shukla S, Peterson P, Wang S, Funk C, Peters-Lidard CD, Verdin JP. 2017. A land data assimilation system for sub-Saharan Africa food and water security applications. *Scientific Data* 4: 170012. <https://doi.org/10.1038/sdata.2017.12>

McNally A, Verdin K, Harrison L, Getirana A, Jacob J, Shukla S, Arsenault K, Peters-Lidard C, Verdin JP. 2019. Acute water-scarcity monitoring for Africa. *Water* 11: 1968. <https://doi.org/10.3390/w11101968>

Motohka T, Nasahara KN, Miyata A, Mano M, Tsuchida S. 2009. Evaluation of optical satellite remote sensing for rice paddy phenology in monsoon Asia using continuous in situ dataset. *International Journal of Remote Sensing* 30: 4343-4357. <https://doi.org/10.1080/01431160802549369>

Mubeen M, Bano A, Ali B, Islam ZU, Ahmad A, Hussain S, Fahad S, Nasim W. 2021. Effect of plant growth promoting bacteria and drought on spring maize (*Zea mays* L.). *Pakistan Journal of Botany* 53: 1-10. [https://doi.org/10.30848/PJB2021-2\(38\)](https://doi.org/10.30848/PJB2021-2(38))

Mynden RB, Keeling CD, Tucker CJ, Asrar G, Nemani RR. 1997. Increased plant growth in the northern high latitudes from 1981 to 1991. *Nature* 386: 698-702. <https://doi.org/10.1038/386698a0>

Nasim W, Amin A, Fahad S, Awais M, Khan N, Mubeen M, Wahid A, Rehman MH, Ihsan MZ, Ahmad S, Hussain S, Mian IA, Khan B, Jamal Y. 2018. Future risk assessment by estimating historical heat wave trends with projected heat accumulation using SimCLIM climate model in Pakistan. *Atmospheric Research* 205: 118-133. <https://doi.org/10.1016/j.atmosres.2018.01.009>

Naz S, Fatima Z, Iqbal P, Khan A, Zakir I, Ullah H, Abbas G, Ahmed M, Mubeen M, Hussain S, Ahmad S. 2022. An introduction to climate change phenomenon. In: *Building climate resilience in agriculture: Theory, practice and future perspective* (Jatoi WN, Mubeen M, Ahmad A, Cheema MA, Lin Z, Hashmi MZ, Eds.). Springer, Cham, 3-16. https://doi.org/10.1007/978-3-030-79408-8_1

Nicholson SE, Davenport ML, Malo AR. 1990. A comparison of the vegetation response to rainfall in the Sahel and East Africa, using normalized difference vegetation index from NOAA AVHRR. *Climatic Change* 17: 209-241. <https://doi.org/10.1007/BF00138369>

Ogutu JO, Piepho HP, Dublin HT, Bhola N, Reid RS. 2008. El Niño-Southern Oscillation, rainfall, temperature and normalized difference vegetation index fluctuations in the Mara-Serengeti ecosystem. *African Journal of Ecology* 46: 132-143. <https://doi.org/10.1111/j.1365-2028.2007.00821.x>

Olmos-Trujillo E, González-Trinidad J, Júnez-Ferreira H, Pacheco-Guerrero A, Bautista-Capetillo C, Ávila-Sandoval C, Galván-Tejada E. 2020. Spatio-temporal response of vegetation indices to rainfall and temperature in a semiarid region. *Sustainability* 12: 1939. <https://doi.org/10.3390/su12051939>

Pelkey NW, Stoner CJ, Caro TM. 2000. Vegetation in Tanzania: Assessing long term trends and effects of protection using satellite imagery. *Biological Conservation* 94: 297-309. [https://doi.org/10.1016/S0006-3207\(99\)00195-0](https://doi.org/10.1016/S0006-3207(99)00195-0)

Peng X, Wu W, Zheng Y, Sun J, Hu T, Wang P. 2020. Correlation analysis of land surface temperature and

topographic elements in Hangzhou, China. *Scientific Reports* 10: 10451. <https://doi.org/10.1038/s41598-020-67423-6>

Philippon N, Jarlan L, Martiny N, Camberlin P, Mougin E. 2007. Characterization of the interannual and intraseasonal variability of West African vegetation between 1982 and 2002 by means of NOAA AVHRR NDVI Data. *Journal of Climate* 20: 1202-1218. <https://doi.org/10.1175/JCLI4067.1>

Piao S, Fang J, Zhou L, Guo Q, Henderson M, Ji W, Li Y, Tao S. 2003. Interannual variations of monthly and seasonal normalized difference vegetation index (NDVI) in China from 1982 to 1999. *Journal of Geophysical Research* 108: 4401. <https://doi.org/10.1029/2002JD002848>

Piao S, Fang J, Zhou L, Ciais P, Zhu B. 2006. Variations in satellite-derived phenology in China's temperate vegetation. *Global Change Biology* 12: 672-685. <https://doi.org/10.1111/j.1365-2486.2006.01123.x>

Piao S, Wang X, Ciais P, Zhu B, Wang T, Liu J. 2011. Changes in satellite-derived vegetation growth trend in temperate and boreal Eurasia from 1982 to 2006. *Global Change Biology* 17: 3228-3239. <https://doi.org/10.1111/j.1365-2486.2011.02419.x>

Potter CS, Brooks V. 1998. Global analysis of empirical relations between annual climate and seasonality of NDVI. *International Journal of Remote Sensing* 19: 2921-2948. <https://doi.org/10.1080/014311698214352>

Rani M, Kumar P, Pandey PC, Srivastava PK, Chaudhary BS, Tomar V, Mandal VP. 2018. Multi-temporal NDVI and surface temperature analysis for urban heat island inbuilt surrounding of sub-humid region: A case study of two geographical regions. *Remote Sensing Application: Society and Environment* 10: 163-172. <https://doi.org/10.1016/j.rsase.2018.03.007>

Richard Y, Poccard I. 1998. A statistical study of NDVI sensitivity to seasonal and interannual rainfall variations in Southern Africa. *International Journal of Remote Sensing* 19: 2907-2920. <https://doi.org/10.1080/014311698214343>

Rocha AV, Shaver GR. 2009. Advantages of a two band EVI calculated from solar and photosynthetically active radiation fluxes. *Agricultural and Forest Meteorology* 149: 1560-1563. <https://doi.org/10.1016/j.agrformet.2009.03.016>

Rouse JW Jr. 1974. Monitoring the vernal advancement and retrogradation (green wave effect) of natural vegetation. *NASA/GSFC Type III Final Report CR-139243*.

Sabr A, Moeinaddini M, Azarnivand H, Guinot B. 2016. Assessment of land use and land cover change using spatiotemporal analysis of landscape: Case study in south of Tehran. *Environmental Monitoring and Assessment* 188: 691. <https://doi.org/10.1007/s10661-016-5701-9>

Saha A, Mitra A, Pal N, Zaman S, Mitra A. 2019. Spatial variation of soil texture in the world heritage site of Indian Sundarbans. *Acta Scientific Microbiology* 2: 120-122. <http://doi.org/10.31080/ASMI.2019.02.0311>

Sahoo RN, Dutta D, Khanna M, Kumar N, Bandyopadhyay SK. 2015. Drought assessment in the Dhar and Mewat districts of India using meteorological hydrological and remote sensing derived indices. *Natural Hazards* 77: 733-751. <https://doi.org/10.1007/s11069-015-1623-z>

Sajedi-Hosseini F, Choubin B, Solaimani K, Cerdá A, Kavian A. 2018. Spatial prediction of soil erosion susceptibility using a fuzzy analytical network process: Application of the fuzzy decision making trial and evaluation laboratory approach. *Land Degradation & Development* 29: 3092-3103. <https://doi.org/10.1002/lrd.3058>

Schwartz MD, Ahas R, Aasa A. 2006. Onset of spring starting earlier across the Northern Hemisphere. *Global Change Biology* 12: 343-351, <https://doi.org/10.1111/j.1365-2486.2005.01097.x>

Sellers PJ, Mintz Y, Sud YC, Dalcher A. 1986. A simple biosphere model (SIB) for use within general circulation models. *Journal of Atmospheric Science* 43: 505-531. [https://doi.org/10.1175/1520-0469\(1986\)043%3C0505:ASBMFU%3E2.0.CO;2](https://doi.org/10.1175/1520-0469(1986)043%3C0505:ASBMFU%3E2.0.CO;2)

Senanayake IP, Welivitiya WDDP, Nadeeka PM. 2013. Remote sensing based analysis of urban heat islands with vegetation cover in Colombo City, Sri Lanka using Landsat-7 ETM+ data. *Urban Climate* 5: 19-35. <https://doi.org/10.1016/j.uclim.2013.07.004>

Sha Z, Bai Y, Lan H, Liu X, Li R, Xie Y. 2020. Can more carbon be captured by grasslands? A case study of Inner Mongolia, China. *Science of The Total Environment* 723: 138085. <https://doi.org/10.1016/j.scitotenv.2020.138085>

Sharma H, Ehlers TA, Glotzbach C, Schmid M, Tielbörger K. 2021. Effect of rock uplift and Milankovitch timescale variations in precipitation and vegetation cover on catchment erosion rates. *Earth Surface Dynamics* 9, 1045-1072. <https://doi.org/10.5194/esurf-9-1045-2021>

Sharma M, Bangotra P, Gautam AS, Gautam S. 2022. Sensitivity of normalized difference vegetation index (NDVI) to land surface temperature, soil moisture and precipitation over district Gautam Buddh Nagar, UP, India. *Stochastic Environmental Research and Risk Assessment*: 1779 - 1789 <https://doi.org/10.1007/s00477-021-02066-1>

Skofronick-Jackson G, Petersen WA, Berg W, Kidd C, Stocker EF, Kirschbaum DB, Kakar R, Braun SA, Huffman GJ, Iguchi T, Kirtstetter PE, Kummerow C, Meneghini R, Oki R, Olson WS, Takayabu YN, Furukawa K, Wilheit T. 2017. The Global Precipitation Measurement (GPM) mission for science and society. *Bulletin of the American Meteorological Society* 98: 1679-1695. <https://doi.org/10.1175/BAMS-D-15-00306.1>

Ssemmanda I, Gelorini, Verschuren D. 2014. Sensitivity of East African savannah vegetation to historical moisture-balance variation. *Climate of the Past* 10: 2067-2080. <https://doi.org/10.5194/cp-10-2067-2014>

Sultana SR, Ali A, Ahmad A, Mubeen M, Zia-Ul-Haq M, Ahmad S, Ercisli S, Jaafar HZE. 2014. Normalized difference vegetation index as a tool for wheat yield estimation: A case study from Faisalabad Pakistan. *The Scientific World Journal* 2014: 725326 <https://doi.org/10.1155/2014/725326>

Tariq A, Riaz I, Ahmad Z, Yang B, Amin M, Kausar R, Andleeb S, Farooqi MA, Rafiq M. 2020. Land surface temperature relation with normalized satellite indices for the estimation of spatio-temporal trends in temperature among various land use land cover classes of an arid Potohar region using Landsat data. *Environmental Earth Science* 79: 40. <https://doi.org/10.1007/s12665-019-8766-2>

Tucker CJ. 1979. Red and photographic infrared linear combinations for monitoring vegetation. *Remote sensing of Environment* 8: 127-150. [https://doi.org/10.1016/0034-4257\(79\)90013-0](https://doi.org/10.1016/0034-4257(79)90013-0)

Tucker CJ, Pinzón JE, Brown ME, Slayback DA, Pak EW, Mahoney R, Vermote EF, Saleous NE. 2005. An extended AVHRR 8-Km NDVI dataset compatible with MODIS and SPOT Vegetation NDVI data. *International Journal of Remote Sensing* 20: 4485-4498. <https://doi.org/10.1080/01431160500168686>

Vélez S, Martínez-Peña R, Castrillo D. 2023. Beyond vegetation: A review unveiling additional insights into agriculture and forestry through the application of vegetation indices. *J* 6: 421-436. <https://doi.org/10.3390/j6030028>

Waleed M, Mubeen M, Ahmad A, Habib-ur-Rahman M, Amin A, Farid HU, Hussain S, Ali M, Qaisrani SA, Nasim W, Javeed HMR, Masood N, Aziz T, Mansour F, El Sabagh A. 2022. Evaluating the efficiency of coarser to finer resolution multispectral satellites in mapping paddy rice fields using GEE implementation. *Scientific Reports* 12: 13210. <https://doi.org/10.1038/s41598-022-17454-y>

Walther GR, Post E, Convey P, Menzel A, Parmesan C, Beebee TJC, Fromentin JM, Hoegh-Guldberg O, Bairlein F. 2002. Ecological responses to recent climate change. *Nature* 416: 389-395. <https://doi.org/10.1038/416389a>

Wan Z. 2006. Collection-5: MODIS land surface temperature products users' guide. Institute for Computational Earth System Science, University of California, Santa Barbara.

Wan Z, Hook S, Hulley G. 2015. MOD11C3 MODIS/Terra Land Surface Temperature/Emissivity Monthly L3 Global 0.05Deg CMG V006 [data set]. NASA EOSDIS Land Processes Distributed Active Archive Center. <https://doi.org/10.5067/MODIS/MOD11C3.006> (accessed 2021 december 18)

Wang J, Rich PM, Price KP. 2003. Temporal responses of NDVI to precipitation and temperature in the central Great Plains, USA. *International Journal of Remote Sensing* 24: 2345-2364. <https://doi.org/10.1080/01431160210154812>

Wang L, Niu S, Good SP, Soderberg K, McCabe MF, Sherry RA, Luo Y, Zhou X, Xia J, Caylor KK. 2013. The effect of warming on grassland evapotranspiration partitioning using laser-based isotope monitoring techniques. *Geochimica et Cosmochimica Acta* 111: 28-38. <https://doi.org/10.1016/j.gca.2012.12.047>

Wu C, Hou X, Peng D, Gonsamo A, Xu S. 2016. Land surface phenology of China's temperate ecosystems over 1999-2013: Spatial-temporal patterns, interaction effects, covariation with climate and implications for productivity. *Agricultural and Forest Meteorology* 216: 177-187. <https://doi.org/10.1016/j.agrformet.2015.10.015>

Xiong S, Johansson ME, Hughes FMR, Hayes A, Richards KS, Nilsson C. 2003. Interactive effects of soil moisture, vegetation canopy, plant litter and seed addition on plant diversity in a wetland community. *Journal of Ecology* 91: 976-986. <https://doi.org/10.1046/j.1365-2745.2003.00827.x>

Yamaguchi T, Kishida K, Nunohiro E, Park JG, Mackin KJ, Hara K, Matsushita KHK, Harada I. 2010.

Artificial neural network paddy-field classifier using spatiotemporal remote sensing data. *Artificial Life and Robotics* 15: 221-224. <https://doi.org/10.1007/s10015-010-0797-4>

Yang X, Yang Q, Zhu H, Wang L, Wang C, Pang G, Du C, Mubeen M, Hussain S. 2023a. Quantitative evaluation of soil water and wind erosion rates in Pakistan. *Remote Sensing* 15: 2404. <https://doi.org/10.3390/rs15092404>

Yang Q, Jiang Q, Ding T. 2023b. Impacts of extreme-high-temperature events on vegetation in North China. *Remote Sensing* 15: 4542. <https://doi.org/10.3390/rs15184542>

Yu F, Price KP, Ellis J, Shi P. 2003. Response of seasonal vegetation development to climatic variations in eastern central Asia. *Remote Sensing of Environment* 87: 42-54. [https://doi.org/10.1016/s0034-4257\(03\)00144-5](https://doi.org/10.1016/s0034-4257(03)00144-5)

Yue W, Xu J, Tan W, Xu L. 2007. The relationship between land surface temperature and NDVI with remote sensing: Application to Shanghai Landsat 7 ETM+ data. *International Journal of Remote Sensing* 28: 3205-3226. <https://doi.org/10.1080/01431160500306906>

Zahoor SA, Ahmad S, Ahmad A, Wajid A, Khaliq T, Mubeen M, Hussain S, Din MSU, Amin A, Awais M, Nasim W. 2019. Improving water use efficiency in agronomic crop production. In: *Agronomic crops. Vol. 2: Management practices* (Hasanuzzaman M, Ed.). Springer, Singapore. https://doi.org/10.1007/978-981-32-9783-8_2

Zhang G, Zhang Y, Dong J, Xiao X. 2013. Green-up dates in the Tibetan Plateau have continuously advanced from 1982 to 2011. *Proceedings of the National Academy of Sciences* 110: 4309-4314. <https://doi.org/10.1073/pnas.1210423110>

Zhang JH, Fu CB, Yan XD, Emori S, Kanzawa H. 2002. A global response analysis of LAI versus surface air temperature and precipitation variations. *Chinese Journal of Geophysics* 45: 662-669, <https://doi.org/10.1002/cjg2.280>

Zhao, X, Zhou D, Fang J. 2012. Satellite based studies on large scale vegetation changes in China F. *Journal of Integrative Plant Biology* 54: 713-728. <https://doi.org/10.1111/j.1744-7909.2012.01167.x>

Zhao Y, Herzschuh U, Li Q. 2015. Complex vegetation responses to climate change on the Tibetan Plateau: A paleoecological perspective. *National Science Review* 2: 400-402. <https://doi.org/10.1093/nsr/nwv057>

Zhe M, Zhang X. 2021. Time-lag effects of NDVI responses to climate change in the Yamzhog Yumco Basin, South Tibet. *Ecological Indicators* 124: 107431. <https://doi.org/10.1016/j.ecolind.2021.107431>